

 Open access • Journal Article • DOI:10.1111/1462-2920.13662

Evolution of copper resistance in the kiwifruit pathogen *Pseudomonas syringae* pv. *actinidiae* through acquisition of integrative conjugative elements and plasmids

— [Source link](#) 

[Elena Colombi](#), [Christina Straub](#), [Sven Künzel](#), [Matthew D. Templeton](#) ...+5 more authors

Institutions: [Massey University](#), [Max Planck Society](#), [University of Auckland](#), [Chinese Academy of Sciences](#) ...+1 more institutions

Published on: 01 Feb 2017 - [Environmental Microbiology](#) (Blackwell Science)

Topics: [Pseudomonas syringae](#)

Related papers:

- [Origin and Evolution of the Kiwifruit Canker Pandemic.](#)
- [Genomic Analysis of the Kiwifruit Pathogen *Pseudomonas syringae* pv. *actinidiae* Provides Insight into the Origins of an Emergent Plant Disease](#)
- [Genome analysis of the kiwifruit canker pathogen *Pseudomonas syringae* pv. *actinidiae* biovar 5.](#)
- [The Scientific, Economic, and Social Impacts of the New Zealand Outbreak of Bacterial Canker of Kiwifruit \(*Pseudomonas syringae* pv. *actinidiae*\).](#)
- [Evolution of copper resistance in the kiwifruit pathogen *Pseudomonas syringae* pv. *actinidiae* through acquisition of integrative conjugative elements and plasmids](#)

Share this paper:    

View more about this paper here: <https://typeset.io/papers/evolution-of-copper-resistance-in-the-kiwifruit-pathogen-erhxhtihm5>

1 **Evolution of copper resistance in the kiwifruit pathogen *Pseudomonas***
2 ***syringae* pv. *actinidiae* through acquisition of integrative conjugative**
3 **elements and plasmids**

4
5 Elena Colombi¹, Christina Straub¹, Sven Künzel², Matthew D. Templeton^{3,4},
6 Honour C. McCann^{1,5*}, Paul B. Rainey^{1,2,6*}

7
8 ¹New Zealand Institute for Advanced Study, Massey University, Auckland, New
9 Zealand. ²Max Planck Institute for Evolutionary Biology, Plön, Germany. ³Plant
10 and Food Research, Auckland, New Zealand. ⁴School of Biological Sciences,
11 University of Auckland, Auckland, New Zealand. ⁵South China Botanical Institute,
12 Chinese Academy of Sciences, Guangzhou, China. ⁶Ecole Supérieure de Physique
13 et de Chimie Industrielles de la Ville de Paris (ESPCI Paris-Tech), PSL Research
14 University, Paris, France. * Joint senior authors

15
16 **Correspondence:** Elena Colombi, New Zealand Institute for Advanced Study,
17 Massey University, Private Bag 102 904, Auckland 0745, New Zealand.
18 Telephone: +64 9 4140800 ext 43810. e-mail: e.colombi@massey.ac.nz

19
20 **Running title:** Evolution of copper resistance

21
22 **ORIGINALITY-SIGNIFICANT STATEMENT**

23 Lateral gene transfer is a major evolutionary force, but its immediacy is often
24 overlooked. Between 2008 and 2010 a single virulent clone of the kiwifruit
25 pathogen *Pseudomonas syringae* pv. *actinidiae* spread to kiwifruit growing

26 regions of the world. After arrival in New Zealand it acquired genetic
27 determinants of copper resistance in the form of integrative conjugative
28 elements and plasmids. Components of these elements are evident in distantly
29 related bacteria from millet (USA, 1921), kiwifruit (Japan, 1988) and wheat (New
30 Zealand, 1968). Additional laboratory experiments capture evidence of the
31 dynamism underpinning the evolution of these elements in real time and further
32 emphasize the potent role that lateral gene transfer plays in microbial evolution.

33

34 **SUMMARY**

35 Lateral gene transfer can precipitate rapid evolutionary change. In 2010 the
36 global pandemic of kiwifruit canker disease caused by *Pseudomonas syringae* pv.
37 *actinidiae* (*Psa*) reached New Zealand. At the time of introduction, the single
38 clone responsible for the outbreak was sensitive to copper, however, analysis of
39 a sample of isolates taken in 2015 and 2016 showed that a quarter were copper
40 resistant. Genome sequences of seven strains showed that copper resistance –
41 comprising *czc/cusABC* and *copABCD* systems – along with resistance to arsenic
42 and cadmium, was acquired via uptake of integrative conjugative elements
43 (ICEs), but also plasmids. Comparative analysis showed ICEs to have a mosaic
44 structure, with one being a tripartite arrangement of two different ICEs and a
45 plasmid that were isolated in 1921 (USA), 1968 (NZ) and 1988 (Japan), from *P.*
46 *syringae* pathogens of millet, wheat and kiwifruit, respectively. Two of the *Psa*
47 ICEs were nearly identical to two ICEs isolated from kiwifruit leaf colonists prior
48 to the introduction of *Psa* into NZ. Additionally, we show ICE transfer *in vitro* and
49 *in planta*, analyze fitness consequences of ICE carriage, capture the *de novo*
50 formation of novel recombinant ICEs, and explore ICE host-range.

51

52 **INTRODUCTION**

53 Horizontal gene transfer (HGT) is a potent evolutionary process that
54 significantly shapes patterns of diversity in bacterial populations. Horizontally
55 transmissible elements, including plasmids, phages and integrative conjugative
56 elements (ICEs) move genes over broad phylogenetic distances and mediate
57 abrupt changes in niche preferences (Sullivan and Ronson, 1998; Ochman *et al.*,
58 2000; Ochman *et al.*, 2005; Guglielmini *et al.*, 2011).

59 ICEs are plasmid-like entities with attributes of temperate phages that
60 disseminate vertically as part of the bacterial chromosome and horizontally by
61 virtue of endogenously encoded machinery for conjugative transfer (Wozniak
62 and Waldor, 2010; Guglielmini *et al.*, 2011). Essential genetic modules include
63 those mediating integration, excision, conjugation and regulation of conjugative
64 activity (Mohd-Zain *et al.*, 2004; Juhas *et al.*, 2007; Roberts and Mullany, 2009).
65 During the process of conjugation ICEs circularize and transfer to new hosts,
66 leaving a copy in the original host genome (Wozniak and Waldor, 2010; Johnson
67 and Grossman, 2015). Conjugation during pathogenesis is often regulated by
68 environmental signals (Lovell *et al.*, 2009; Quiroz *et al.*, 2011; Vanga *et al.*, 2015).

69 In addition to a set of essential genes, ICEs often harbour “cargo” genes of
70 adaptive significance to their hosts. These include genes affecting biofilm
71 formation, pathogenicity, antibiotic and heavy metal resistance, symbiosis and
72 bacteriocin synthesis (Peters *et al.*, 1991; Rauch *et al.*, 1992; Ravatn *et al.*, 1998;
73 Beaber *et al.*, 2002; Drenkard *et al.*, 2002; Burrus *et al.*, 2006; Ramsay *et al.*,
74 2006; Dimopoulou *et al.*, 2007; Kung *et al.*, 2010). The genetic information stored
75 in cargo genes varies considerably causing ICEs to range in size from 20 kb to

76 500 kb (Johnson and Grossman, 2015).

77 In 2008 a distinct and particularly virulent form of the kiwifruit pathogen
78 *Pseudomonas syringae* pv. *actinidiae* (*Psa*) was identified in Italy. It was
79 subsequently disseminated throughout kiwifruit growing regions of the world
80 causing a global pandemic that reached New Zealand (NZ) in 2010 (Balestra *et*
81 *al.*, 2010; Abelleira *et al.*, 2011; Everett *et al.*, 2011; Vanneste *et al.*, 2011).

82 Genomic analysis showed that although the pandemic was derived from a single
83 clone it acquired a set of distinctive ICEs during the course of its global journey
84 (Mazzaglia *et al.*, 2012; Butler *et al.*, 2013; McCann *et al.*, 2013). The NZ lineage
85 carries *Psa*_{NZ13}ICE_eno which harbours a 20 kb “enolase” region that is also
86 found in otherwise divergent *Psa* ICEs (McCann *et al.*, 2013; McCann *et al.*, 2016).

87 Copper sprays have long been used in NZ to protect plants from a range of
88 diseases. Since the arrival *Psa* in NZ kiwifruit orchardists have employed copper
89 based products to protect vines. From 2011 an ongoing industry-based
90 programme has been in place to monitor copper resistance. In 2014 evidence
91 was first obtained of *Psa* isolates resistant to copper sulphate. Given that the
92 clone of *Psa* originally introduced into NZ was sensitive to copper and lacked
93 genes encoding copper resistance (McCann *et al.*, 2013), detection of copper
94 resistance raised the possibility that the evolution of copper resistance in *Psa* is
95 an evolutionary response to the use of copper-based sprays.

96 Here we report the phenotypic and genetic basis of copper resistance in
97 NZ isolates of *Psa* and show that its emergence has been fuelled by lateral gene
98 transfer involving ICEs and plasmids. We additionally describe the mosaic
99 structure of ICEs, show the dynamics of ICE transfer both *in vitro* and *in planta*,

100 analyze fitness consequences of ICE carriage, capture the *de novo* formation of
101 novel recombinant ICEs, and explore ICE host-range.

102

103 **RESULTS**

104 **Occurrence of copper resistance in *Psa***

105 *Psa* NZ13, isolated in 2010 and representative of the clone introduced in
106 New Zealand, lacks genes encoding copper resistance (McCann *et al.*, 2013) and
107 is unable to grow at copper concentrations in excess of 0.8 mM CuSO₄. Prior to
108 2014 no copper resistant or tolerant strains had been reported. However, in
109 2014, two strains isolated from two different kiwifruit orchards, *Psa* NZ45 and
110 *Psa* NZ47, displayed copper resistance, with a MIC of 1.2 mM CuSO₄. This finding
111 prompted a small-scale sampling of both copper treated and untreated orchards
112 in 2015/2016 encompassing the area where resistance was first identified. From
113 a sample of 213 strains isolated from seven orchards 59 were found to be copper
114 resistant. Copper resistant isolates were sampled from both copper treated and
115 untreated orchards. Additional copper resistant strains were procured from
116 other kiwifruit-growing regions of New Zealand (Figure S1).

117

118 **ICE and plasmid-mediated acquisition of copper resistance in *Psa***

119 The genome of the focal copper resistant isolate, *Psa* NZ45, is a direct
120 clonal descendant of the isolate originally introduced into NZ (*Psa* NZ13)
121 (McCann *et al.*, 2016), but differs in two significant regards. Firstly, the “native”
122 ICE (*Psa*_{NZ13}ICE_eno) at *att*-1 (immediately upstream of *clpB*), is located at the
123 second *att* site (*att*-2) immediately downstream of *queC* (Figure 1). Secondly, the

124 genome harbours a new 107 kb ICE (*Psa*_{NZ45}ICE_Cu) integrated at the *att-1* site:
125 *Psa*_{NZ45}ICE_Cu carries genes encoding copper resistance (Figures 1 and 2A).
126 The genomes of six additional copper resistant *Psa* isolates were also
127 sequenced (Table 1) and as with *Psa* NZ45, reads were aligned against the *Psa*
128 NZ13 reference genome (McCann *et al.*, 2013; Templeton *et al.*, 2015). All six
129 harbour mobile elements carrying genes encoding copper resistance. The
130 diversity of these elements and genomic location is shown in Figure 1 and their
131 structure is represented in Figure 2A. All isolates are direct clonal descendants of
132 *Psa* NZ13 and thus share an almost identical genome with the exception of the
133 determinants of copper resistance. In *Psa* NZ47 the genes encoding copper
134 resistance are located on a 90 kb ICE (*Psa*_{NZ47}ICE_Cu) integrated at the *att-1* site:
135 the native *Psa*_{NZ13}ICE_eno is located at the *att-2* site. *Psa* NZ62 carries an ICE
136 identical to that found in *Psa*_{NZ47}ICE_Cu (*Psa*_{NZ62}ICE_Cu), but is integrated at the
137 *att-2* site; the native ICE (*Psa*_{NZ13}ICE_eno) is absent leaving the *att-1* site
138 unoccupied. Isolate *Psa* NZ63 carries *Psa*_{NZ45}ICE_Cu integrated at the *att-1* site,
139 but as in *Psa* NZ62, the native *Psa*_{NZ13}ICE_eno has been lost. Copper resistance
140 genes in isolate *Psa* NZ64 are also ICE-encoded, but the NZ64 ICE
141 (*Psa*_{NZ64}ICE_Cu) is genetically distinct from both *Psa*_{NZ47}ICE_Cu and
142 *Psa*_{NZ45}ICE_Cu – at 130 kb, it is also the largest. In NZ64, *Psa*_{NZ64}ICE_Cu is located
143 at the *att-1* site and the *att-2* site contains the native (*Psa*_{NZ13}ICE_eno) ICE.
144 Isolates *Psa* NZ65 and NZ66 both harbour copper resistance genes on a near
145 identical, 120 kb previously undescribed plasmid (p*Psa*_{NZ65} and p*Psa*_{NZ66},
146 respectively). The only significant difference among the plasmids is the location
147 of a streptomycin resistance-encoding transposon (see below): both isolates have
148 the original *Psa*_{NZ13}ICE_eno integrated at the *att-2* site (Figure 1). *Psa* harbouring

149 copper resistance-encoding ICEs have a MIC CuSO₄ of 1.2 mM while the MIC of
150 plasmid-carrying *Psa* 1.5 mM (Table 1).

151 That such a small sample of isolates is each unique with regard to the
152 copper resistance-encoding element points to highly dynamic processes shaping
153 their evolution. Such dynamism has been previously noted among enolase-
154 encoding ICEs obtained from a global collection of epidemic *Psa* isolates
155 (McCann *et al.*, 2013) and has been observed elsewhere (Burrus *et al.*, 2006,
156 Wozniak and Waldorf, 2010). In this study our samples came from a relatively
157 small geographical location. Two ICEs, *Psa*_{NZ64}ICE_Cu and *Psa*_{NZ47}ICE_Cu were
158 found in different isolates sampled from the same orchard (one year apart),
159 although the two isolates containing near identical plasmids were isolated from
160 orchards located 100 km apart. Two isolates sampled one year apart from the
161 same location (neighboring orchards in Te Puke) carry the same ICE
162 (*Psa*_{NZ45}ICE_Cu=*Psa*_{NZ63}ICE_Cu; *Psa*_{NZ47}ICE_Cu=*Psa*_{NZ62}ICE_Cu) (Table 1).

163 The dynamics of ICE evolution becomes especially evident when placed in
164 the broader context possible by comparisons to ICEs recorded in DNA databases.
165 The core genes of the copper resistance-encoding ICEs from New Zealand *Psa*
166 isolates are syntenous with the core genes of the family of ICEs that includes
167 PPHGI-1 (isolated in 1984 from bean in Ethiopia (Teverson, 1991; Pitman *et al.*,
168 2005) and the three ICEs previously described from *Psa* found in New Zealand
169 (2010), Italy (2008) and China (2010) (McCann *et al.*, 2013; Butler *et al.*, 2013; E.
170 Colombi, unpublished). *Psa*_{NZ45}ICE_Cu is a mosaic of DNA from two known ICEs
171 and a plasmid. It shares regions of near perfect identity (over 66 kb) with ICEs
172 present in the otherwise divergent host genomes of *P. syringae* *pv.* *panici* (*Ppa*,
173 LGM2367) isolated from proso millet in Madison (USA) in the 1920s (over the

174 first 38 kb it differs by just 12 SNPs, and one 144 bp insertion), *P. syringae* pv.
175 *atrofasciens* (*Paf*, ICMP4394) isolated in NZ in 1968 from wheat, and a 70.5 kb
176 plasmid present in a non-pandemic *Psa* strain (J2), isolated in Japan in 1988
177 (Figure 2B).

178 Interestingly, two of the ICEs described here have also been found in non-
179 *Psa Pseudomonas* isolated from kiwifruit leaves. *Psa_{NZ47}ICE_Cu* shows 99.7%
180 pairwise nucleotide identity with an ICE found in *P. marginalis* ICMP 11289
181 isolated in 1991 from *A. deliciosa* in Katikati (New Zealand). *Psa_{NZ64}ICE_Cu* is
182 almost identical (99.5% nucleotide pairwise identity) to an ICE from *P. syringae*
183 pv. *actinidifoliorum* (*Pfm*) ICMP19497, isolated from kiwifruit in 2010 in Te Puke
184 (New Zealand) (Visnovsky *et al.*, 2016) (Table 1). Additionally, a 48 kb segment
185 of coding copper resistance genes *Psa_{NZ64}ICE_Cu* shares 99.3% nucleotide
186 pairwise identity with a locus found in *P. azotoformans* strain S4 (Fang *et al.*,
187 2016), which was isolated from soil in 2014 in Lijiang (China). However, the
188 locus from *P. azotoformans* is not associated with an ICE.

189

190 **Genetic determinants of copper resistance**

191 Copper resistance is typically conferred by operons encoding either
192 copper efflux (*cusABC*) and / or sequestration (*copABCD*) systems, both of which
193 can be under the regulation of the *copRS* / *cusRS* two-component regulatory
194 system (Bondarczuk and Piotrowska-Seget, 2013). ICEs identified in *Psa* isolates
195 harbour operons encoding examples of both resistance mechanisms (and
196 regulators), plus genetic determinants of resistance to other metal ions. In each
197 instance the resistance genes are located within “variable regions” (VR) of ICEs
198 into which cargo genes preferentially integrate (Figure 2A). Delineation of these

199 variable regions comes from detailed analysis of 32 unique ICEs from the *Pph*
200 1302A and *Psa* families that will be published elsewhere (E. Colombi,
201 unpublished). Overall there are notable similarities and differences in the
202 organization of the variable regions.

203 As shown in Figure 2B, the first 38 kb of *Psa*_{NZ45}ICE_Cu is almost identical
204 (99.7% identical at the nucleotide level) to *Ppa*_{LGM2367}ICE. This region spans the
205 core genes, but extends ~8.2 kb into the variable cargo genes with just two SNPs
206 distinguishing the two ICEs (across the 8.2 kb variable region). Encoded within
207 this region is an integrase, arsenic resistance genes (*arsRBCH*), a gene implicated
208 in cadmium and cobalt resistance (*czcD*) and the *copRS* regulatory system.
209 Partway through *copS* the two ICEs diverge at a recombination breakpoint with
210 the downstream variable region from *Psa*_{NZ45}ICE_Cu being homologous to a set of
211 copper resistance genes found on plasmid pPaCu1 from the divergent (non-
212 pandemic) Japanese isolate of *Psa* (J2) (Nakajima *et al.*, 2002). This region
213 comprises a putative copper transporting ATPase encoded by *copG* (Gutiérrez-
214 Barranquero *et al.*, 2013), *cusABC* genes involved in the detoxification of
215 monovalent cations, including copper and silver (Mergeay *et al.*, 2003; Rensing
216 and Grass, 2003) and *copABCD* (Figure 2B). The last 4 kb of the variable region of
217 *Psa*_{NZ45}ICE_Cu shares almost complete identity with *Ppa*_{LGM2367}ICE (Figure 2B).

218 Detail of the diversity of copper resistance (and related metal resistance)
219 genes is shown in Figure 3. All elements (ICEs and plasmids) harbour the *copRS*
220 regulatory system and, with the exception of *Psa*_{NZ47}ICE_Cu, all carry both *cusABC*
221 and *copABCD*, although their organization varies. For example, while *copABCD* is
222 typical, in *Psa*_{NZ64}ICE_Cu *copAB* and *copCD* are organized as two separate
223 operons (Figure 3). The putative copper ABC transport system encoded by *copG*

224 is a common feature, and determinants of arsenic resistance are present in both
225 *Psa_{NZ45}ICE_Cu* and *Psa_{NZ64}ICE_Cu*. The putative cadmium and related metal
226 resistance gene, *czcD* is also present on these two ICEs. As noted above, a
227 transposon carrying determinants of streptomycin resistance (*strAB*) is present
228 on plasmids pPsaNZ65 and pPsaNZ66. The transposon is of the Tn3 family and
229 the cassette bears identity to streptomycin resistance carrying transposons
230 found in *P. syringae* pv. *syringae* B728a (Feil *et al.*, 2005), but also on plasmid
231 pMRVIM0713 from *Pseudomonas aeruginosa* strain MRSN17623 (GenBank:
232 KP975076.1), plasmid pPMK1-C from *Klebsiella pneumoniae* strain PMK1
233 (Stoesser *et al.*, 2014), and plasmid pTi carried by *Agrobacterium tumefaciens*
234 LBA4213 (Ach5) (GenBank: CP007228.1).

235 At the level of the operons determining copper resistance there is marked
236 genetic diversity, however, with the exception of CopR, there is relatively little
237 evidence of within operon recombination. The CusABC system is carried on
238 pPsaNZ65 and pPsaNZ66 (but these are identical) and the ICEs *Psa_{NZ45}ICE_Cu*
239 and *Psa_{NZ64}ICE_Cu*: CusA, CusB and CusC show 75.8%, 50.0% and 44.8% pairwise
240 amino acid identity, respectively; phylogenetic trees based on protein sequences
241 show congruence (Figure S2). The CopABCD system is present on *Psa_{NZ45}ICE_Cu*,
242 *Psa_{NZ47}ICE_Cu*, *Psa_{NZ64}ICE_Cu* (but CopAB and CopCD are in different locations
243 (Figure 3)) and plasmid pPsaNZ65 (and pPsaNZ66): CopA, CopB, CopC and CopD
244 show 76.4%, 63.1%, 79.1% and 60.8% pairwise amino acid identity,
245 respectively. With the exception of CopC (where bootstrap support is low)
246 phylogenetic trees for each protein show the same overall arrangement (Figure
247 S3). The two component regulatory system *copRS* is also present on each of the
248 elements with the amino acid sequences of CopR showing 84.3% and those of

249 CopS 63.0% pairwise amino acid identity. Phylogenetic trees show CopS from
250 *Psa*_{NZ64}ICE_Cu to be the most divergent, and those from *Psa*_{NZ45}ICE_Cu and
251 *Psa*_{NZ47}ICE_Cu being most similar: CopR shows the same phylogenetic
252 arrangement, however, CopR sequences from *Psa*_{NZ45}ICE_Cu and *Psa*_{NZ47}ICE_Cu
253 are identical at the protein level suggesting a recent recombination event (Figure
254 S4).

255

256 ***Psa*_{NZ45}ICE_Cu imposes no detectable fitness cost and confers a selective**
257 **advantage *in vitro* in the presence of copper**

258 To determine whether ICE carriage confers a fitness cost, we took
259 advantage of the fact that *Psa* NZ13 and *Psa* NZ45 are essentially isogenic, with
260 the exception of the additional ICE in *Psa* NZ45 (*Psa*_{NZ45}ICE_Cu). Each strain was
261 grown alone and density of cells monitored over a 72 hour period with samples
262 taken every 24 hours. In the absence of copper sulphate, no difference in cell
263 density was detected; however, in the presence of 0.5 and 0.8 mM CuSO₄ the
264 density of *Psa* NZ13 was reduced (Figure 4A). There is thus no apparent fitness
265 cost associated with carriage of *Psa*_{NZ45}ICE_Cu in the absence of copper sulphate,
266 but there is a fitness advantage in copper-containing environments.

267 Although carriage of *Psa*_{NZ45}ICE_Cu appeared not to affect the growth of
268 *Psa* NZ45 in the absence of copper, a more precise measure of fitness was sought
269 by performing competition experiments in which *Psa* NZ13 and *Psa* NZ45 were
270 co-cultured. For this experiment *Psa* NZ13 was marked with a kanamycin
271 resistance cassette so that it could be distinguished from kanamycin sensitive,
272 copper resistant *Psa* NZ45. Over a 24 hour period where the two strains
273 (founded at equal density) competed for the same resources (in shaken MGY

274 medium without copper sulphate), the fitness of *Psa* NZ45 was not significantly
275 different to *Psa* NZ13 (1.07 ± 0.04 ; mean and SEM from 3 independent
276 experiments, each comprised of 3 replicates), indicating no significant detectable
277 cost of carriage of *Psa*_{NZ45}ICE_Cu.

278 Given that the mechanism of copper resistance in *Psa* NZ45 – based upon
279 *copABCD* – likely involves sequestration of copper ions we considered the
280 possibility that this isolate might confer cross protection to non-copper resistant
281 isolates, such as *Psa* NZ13. To this end we performed co-culture experiments at
282 sub-inhibitory and inhibitory copper sulphate concentrations. Growth of *Psa*
283 NZ13 at sub-inhibitory concentrations of copper sulphate was significantly
284 impaired by the presence of *Psa* NZ45 and this was especially evident at 48 and
285 72 hours (Figure S5). At the inhibitory copper sulphate concentration, *Psa* NZ13
286 appeared to benefit from the presence of *Psa* NZ45. Again, this was most evident
287 at 48 and 72 hours (Figure S5).

288

289 ***Psa*_{NZ45}ICE_Cu imposes no detectable fitness cost and confers no selective**
290 **advantage *in planta***

291 Cost and benefit of carrying *Psa*_{NZ45}ICE_Cu was also evaluated during
292 endophytic colonization of kiwifruit leaves. No significant difference was
293 observed in growth of singly-inoculated *Psa* NZ13 and NZ45 (dip inoculation was
294 used to found colonization). Spray application of a commonly used commercial
295 copper-based treatment (Nordox75 (0.375 g L⁻¹)) subsequent to dip inoculation
296 resulted in a reduction of bacterial density of both strains and the presence of
297 *Psa*_{NZ45}ICE_Cu in *Psa* NZ45 did not confer any advantage *in planta* (Figure 4B).
298 Co-cultivation competition assays in the presence or absence of Nordox75

299 confirmed carriage of *Psa*_{NZ45}ICE_Cu imposes no significant fitness cost or
300 advantage during endophytic growth: fitness of NZ45 relative to NZ13 was 1.00
301 ± 0.02 and 1.07 ± 0.03 at day 3 and 7, respectively; fitness of NZ45 relative to
302 NZ13 in the presence of 0.375 g L^{-1} Nordox was 1.15 ± 0.04 and 0.97 ± 0.09 at
303 day 3 and 7, respectively (data are means and SEM from 3 independent
304 experiments, each comprised of 5 replicates; significance was calculated by one
305 sample *t*-test).

306

307 ***Psa*_{NZ45}ICE_Cu transfer dynamics *in vitro* and *in planta***

308 Acquisition of *Psa*_{NZ45}ICE_Cu (and related ICEs) by *Psa* NZ13 suggests that
309 the element is active and capable of self-transmission. If so, then it is possible
310 that transfer may have occurred during the course of the co-cultivation
311 experiments used to determine cost of ICE carriage. To determine whether this
312 had happened samples from the mixtures were plated on MGY medium
313 containing both kanamycin and copper sulphate. Copper resistant, kanamycin
314 resistant transconjugants were detected both *in vitro* and *in planta*. This means
315 that a fraction of *Psa* NZ13 strains acquired *Psa*_{NZ45}ICE_Cu. These
316 transconjugants marginally inflate the counts of *Psa* NZ45, however, the number
317 of transconjugants (see below) was several orders of magnitude less than *Psa*
318 NZ13, thus having no appreciable effect on the measures of relative fitness.

319 At 24 hours in shaken MGY broth transconjugants were present at a
320 frequency of $5.04 \pm 2.25 \times 10^{-3}$ per recipient cell (mean and SEM from 3
321 independent experiments, each comprised of 3 replicates). Analysis of samples
322 from *in planta* experiments showed that at 3 days, transconjugants were present
323 at a frequency of $2.05 \pm 0.63 \times 10^{-2}$ per recipient cell (mean and SEM from 3

324 independent experiments, each comprised of 5 replicates). On plants in the
325 presence of Nordox (0.375 g L^{-1}) the frequency of transconjugants was $9.37 \pm$
326 1.56×10^{-2} per recipient three days after inoculation (mean and SEM from 3
327 independent experiments, each comprised of 5 replicates). Transfer was also
328 observed in M9 agar, on M9 agar supplemented with 0.5 mM CuSO_4 , on M9 agar
329 supplemented with a macerate of Hort16A fruit with transconjugants present (at
330 48 hours) at a frequency of $2.16 \pm 0.9 \times 10^{-5}$, $1.11 \pm 0.4 \times 10^{-5}$ and $1.98 \pm 0.8 \times 10^{-5}$
331 per recipient cell, respectively.

332 To explore the dynamics of transfer *in vitro*, samples from shaken MGY
333 cultures were taken hourly, for six hours, and then at 24 hours. The data,
334 presented in Figure 5, show acquisition of *Psa*_{NZ45}ICE_Cu by *Psa* NZ13 within one
335 hour of the mating mix being established (approximately 1 recipient per 10^5
336 recipient cells). The frequency was relatively invariant over the subsequent six
337 hour period, but rose to approximately 1 recipient in 10^3 cells at 24 hours.

338 Detection of ICE transfer just one hour after mixing donor and recipient
339 cells promoted a further experiment in which transconjugants were assayed at
340 10 minute intervals. From three independent experiments, each with five
341 replicates, transconjugants were detected at 30 mins (approximately 4×10^{-7}
342 transconjugants per recipient cell).

343 Analysis of co-cultivation experiments from kiwifruit leaves showed
344 evidence that *Psa*_{NZ45}ICE_Cu also transferred *in planta*. The frequency of
345 transconjugants at day 3 and day 7 was approximately 1 per 50 recipient cells
346 and the frequency of transconjugants was not affected by changes in the initial
347 founding ratios of donor and recipient cells (Table S1). Overall, the frequency of

348 transconjugants was approximately three orders of magnitude greater *in planta*
349 than *in vitro*.

350

351 **ICE displacement and recombination**

352 To check the genetic composition of transconjugants and to investigate
353 whether *Psa*_{NZ45}ICE_Cu integration in recipient cells occurred at the *att-1* or *att-2*
354 site, a set of primers were designed to identify the location of ICE integration in
355 the *Psa* NZ13 genome (Table S2). 11 independently generated transconjugants
356 from shaken MGY culture were screened. As expected, successful amplification of
357 primers annealing to *copABCD* in *Psa*_{NZ45}ICE_Cu was observed in all
358 transconjugants, while amplification of the *enolase* gene primers (indicative of
359 the presence of the native *Psa*_{NZ13}ICE_eno) occurred only in *Psa* NZ13 and *Psa*
360 NZ45 (Figure S6). However, in two transconjugants only the *IntPsaNZ13-att-1*
361 primer pair resulted in amplification, suggesting that recombination between
362 *Psa*_{NZ45}ICE_Cu and *Psa*_{NZ13}ICE_eno had occurred (Figure S7). Genome sequencing
363 of one of these transconjugants revealed a recombination event inside the
364 variable region of the ICE that produced a chimeric ICE identical to *Psa*_{NZ45}ICE_Cu
365 up to and including the CuR operon, with the remainder identical to the
366 downstream segment of *Psa*_{NZ13}ICE_eno (Figure 6).

367

368 ***Psa*_{NZ45}ICE_Cu can be transferred to a range of *P. syringae* strains**

369 The host range of the *Psa*_{NZ45}ICE_Cu was characterised using a panel of
370 nine different *Pseudomonas* strains as recipients, representing the diversity of *P.*
371 *syringae* and the genus more broadly. Transfer of *Psa*_{NZ45}ICE_Cu to *Psa* J31, *Pfm*
372 NZ9 and *P. syringae* pv. *phaseolicola* (*Pph*) 1448a (on M9 agar plates) was

373 observed with the frequency of transconjugants per recipient cell being $7.64 \pm$
374 1.7×10^{-6} , $7.74 \pm 2.5 \times 10^{-7}$ and $1.23 \pm 0.2 \times 10^{-4}$, respectively. No transconjugants
375 were detected for *P. aeruginosa* PAO1, *P. fluorescens* SBW25, *P. syringae* pv.
376 *tomato* DC3000 or *Psa* K28, despite the fact that these three strains have both *att*
377 sites.

378

379 **DISCUSSION**

380 The importance and impact of lateral gene transfer on the evolution of
381 microbial populations has long been recognized (Sullivan *et al.*, 1995; Lilley and
382 Bailey, 1997; Ochman *et al.*, 2000; Ochman *et al.*, 2005; Wozniak and Waldor,
383 2010; Polz *et al.*, 2013). Here we have captured the real time evolution of copper
384 resistance in a plant pathogen, in an agricultural setting, and shown that
385 movement of copper resistance genes occurs primarily via ICEs. The strains
386 subject to genomic analysis provide a glimpse of just how dynamic evolution
387 fuelled by ICEs can be. Of the seven copper resistant *Psa* isolates analyzed, five
388 contain copper resistance-encoding ICEs – three unique ICEs in total – with
389 variable placement within the *Psa* genome, including movement and instability
390 of the native ICE (*Psa*_{NZ13}ICE_eno). Further evidence of dynamism comes from *in*
391 *vitro* and *in planta* studies, which show not only transfer to isogenic *Psa* and
392 unrelated *P. syringae* strains, but also the ready formation of chimeras between
393 *Psa*_{NZ45}ICE_Cu and *Psa*_{NZ13}ICE_eno. Mosaicism of ICEs has been reported
394 elsewhere and is often promoted by the presence of tandem copies (Garriss *et al.*,
395 2009; Wozniak and Waldor, 2010). The ease with which ICEs move between
396 strains and capacity for intra-ICE recombination emphasizes the futility of
397 drawing conclusions on strain phylogeny based on ICE phylogeny (McCann *et al.*,

398 2013), but also the impossibility of understanding ICE evolution based on the
399 phylogeny of ICEs themselves.

400 Evidence of the formation of chimeric ICEs extends beyond the ICEs
401 studied here. *Psa*_{NZ45}ICE_Cu is a recombinant of two previously reported ICEs
402 and a plasmid: most surprising is the fact that the recombinant components are
403 derived from elements isolated from three geographic regions (USA, Japan and
404 New Zealand) from three different plants (millet, kiwifruit and wheat) and
405 spanning almost 100 years. Additionally, two of the copper resistance-encoding
406 ICEs found in *Psa* (*Psa*_{NZ47}ICE_Cu and *Psa*_{NZ64}ICE_Cu) have been reported in other
407 kiwifruit leaf colonizing organisms emphasizing the ease by which self-
408 transmissible elements can move between members of a single community.
409 Clearly the potency of evolution fuelled by ICEs with the *P. syringae* complex is
410 remarkable, with impacts likely extending well beyond that inferred from the
411 analysis of genome sequences (Fondi *et al.*, 2016).

412 Evidence of the spectrum and dynamic of transfer inferred from the
413 genomic analysis of natural isolates is bolstered by demonstration of the *in vitro*
414 and *in planta* transfer of *Psa*_{NZ45}ICE_Cu. The fact that *Psa*_{NZ45}ICE_Cu can be
415 detected in a recipient strain just 30 minutes after mixing with a donor strain (in
416 shaken broth culture) points to an as yet undetermined proficiency for transfer
417 and possible regulatory mechanism. At the same time, the frequency of
418 transconjugants *in planta* are several orders of magnitude greater than *in vitro*
419 suggesting even greater potential (perhaps regulated) for transfer in the natural
420 environment.

421 The selective causes underpinning the evolution of copper resistance in
422 *Psa* is uncertain and to date copper resistance is not known to have evolved

423 outside of New Zealand. While it is tempting to blame use of copper sprays by
424 orchardists, it is possible that the evolution of copper resistant *Psa* is a more
425 general response to copper levels in New Zealand soils combined with long-term
426 use of copper-based sprays in New Zealand agriculture (Morgan and Taylor,
427 2004). Support for this stems from the fact that *Psa*_{NZ47}ICE_Cu shows almost
428 perfect identity with an ICE found in *P. marginalis* (ICMP 11289) from kiwifruit
429 isolated in 1991 (in New Zealand). In addition, copper resistance-encoding ICEs
430 were found in both copper treated, and untreated orchards. There is need to
431 understand further the population ecology of copper-resistance ICEs at regional,
432 national and global scales and the selective causes for their maintenance and
433 spread (Staehlin *et al.*, 2016).

434 The impact of the copper resistance-encoding ICEs on fitness *in planta* –
435 in the presence of copper sprays – appears to be minimal. While this is
436 heartening news from the perspective of control of the pathogen, there are at
437 least three reasons to treat this result with caution. Firstly, it is difficult to
438 accurately assess fitness *in planta* and it is possible that our measures
439 underestimate the contribution of copper resistance to growth in the presence of
440 copper: even a 1% increase in fitness over 24 hours, which is beyond
441 experimental capacity to detect, can have significant long-term consequences.
442 Secondly, the presence of copper resistance genes means opportunity for levels
443 of resistance to increase through, for example, promoter mutations that increase
444 levels of transcription of resistance determinants, or through acquisition of
445 additional copper resistance-encoding genes. Thirdly, and perhaps most
446 significantly, is the fact that the copper resistance-encoding ICEs confer no
447 measurable fitness cost even in the absence of copper. This suggests that these

448 elements will not be readily lost from *Psa* populations even if copper-based
449 sprays were eliminated (Andersson and Hughes, 2010; Neale *et al.*, 2016). That
450 some strains of the global pandemic now contain two ICEs gives reason to
451 suspect elevated evolutionary potential among these isolates.

452 While the focus of our investigation has been copper resistance, the ICEs
453 reported here carry a cargo of additional genes, some of which are implicated in
454 resistance to other metals. In some instances the cargo genes have no similarity
455 to genes of known function (grey boxes in Figure 2A). ICEs and similar laterally
456 transferred elements provide opportunity for genes unrelated to copper
457 resistance, for example gene connected to virulence, to hitchhike and rapidly
458 spread. In this regard the two plasmids characterized here are of interest: both
459 carry determinants of streptomycin resistance – an antibiotic that is also sprayed
460 on New Zealand kiwifruit orchards in order to control *Psa*. The potential for
461 hitchhiking has been previously noted in the context of antibiotic resistance-
462 encoding plasmids (Gullberg *et al.*, 2014).

463 Recognition of ICEs along with their potential to change the course of
464 microbial evolution extends less than twenty years (Wozniak and Waldor, 2010).
465 While it might be argued that this potential is no different from that long realized
466 via conjugative plasmids, or phage (Ochman *et al.*, 2000), ICEs, being a composite
467 of both, seem to have an edge. Unlike conjugative plasmids that rarely integrate
468 into the host genome, ICEs integrate as a matter of course and are largely
469 immune to segregational loss; additionally, fitness consequences as a result of
470 carriage are likely to be minimal. Unlike temperate phages, ICEs do not kill the
471 host upon transfer, but they can nonetheless mediate transfer upon
472 encountering transfer proficient conditions. Having control over both vertical

473 and horizontal modes of transmission, while minimizing costs for host cells,
474 marks these elements as especially potent vehicles of microbial evolution.

475

476 **EXPERIMENTAL PROCEDURES**

477 **Strains and culture condition**

478 All *Pseudomonas* strains were cultured in King's B medium at 28°C, *E. coli*
479 was cultured in Luria Bertani medium at 37°C. All liquid overnight cultures were
480 shaken at 250 rpm. Both kanamycin and nitrofurantoin were used at 50 µg mL⁻¹.

481

482 **DNA extraction and genome sequencing**

483 For genome sequencing, DNA samples were extracted using the Promega
484 Wizard® Genomic DNA Purification Kit following the recommended protocol.

485 *Psa* NZ45 was sequenced using the PacBio platform, the remainder were
486 sequenced using the Illumina HiSeq platform. Sequences are deposited at NCBI
487 with the following accession numbers: XXXX1, XXXX2 etc (right number of
488 accession numbers).

489

490 **Genomic reconstruction of ICEs**

491 ICEs identified in genome sequences were used as query sequences for
492 BLAST searches of the NCBI WGS database

493 (<http://blast.ncbi.nlm.nih.gov/Blast.cgi>). Contigs were subsequently

494 downloaded and where ICEs were represented by two contigs they were

495 concatenated in Geneious (<http://www.geneious.com>, Kearse *et al.*, 2012).

496 Concatenation was only required in two instances. ICEs were annotated using

497 the RAST server (<http://rast.nmpdr.org>, Aziz *et al.*, 2008) and manually curated.

498 Alignments were performed using Geneious.

499

500 ***Psa* isolation from kiwifruit orchards**

501 One cm² kiwifruit leaf disks were macerated in 200 µl 10mM MgCl₂. The
502 macerate was plated on *Pseudomonas* selective media amended with cetrimide,
503 fucidin and cephalosporin (Oxoid) and incubated at 28°C for 3 days. *Psa* was
504 identified using either diagnostic PCR or LAMP assays (Rees-George *et al.*, 2010,
505 Ruinelli *et al.*, 2016).

506

507 **Copper resistance assays**

508 Copper resistance was evaluated by determining the minimal
509 concentration of copper that inhibited growth (minimal inhibitory
510 concentration, MIC) on mannitol-glutamate yeast extract medium (MGY) plates
511 supplemented with CuSO₄·5H₂O (Bender and Cooksey, 1986, Cha and Cooksey
512 1991). *Psa* strains were considered resistant when their MIC exceeded 0.8 mM
513 CuSO₄.

514

515 **Mutant development**

516 A Tn5 transposon was used to generate kanamycin resistant (*kanR*)
517 strains. *E. coli* S17-1 Tn5*hah Sgid1* (Zhang *et al.*, 2015) was used as donor and *E.*
518 *coli* pK2013 (Ditta *et al.*, 1980) as helper. Helper, donor and recipients were
519 grown overnight. 200 µl of helper and donor and 2 mL of recipient were
520 separately washed with 10mM MgCl₂ and then mixed together and washed
521 again. The mix was then re-suspended in 30 µl of 10 mM MgCl₂, plated on pre-

522 warmed LB agar plates and incubated for 24-48 hours at 28°C. Cells were then
523 harvested, resuspended in 1ml of sterile 10 mM MgCl₂ and plated on KB
524 kanamycin nitrofurantoin plates. Selected mutants were screened for normal
525 growth in KB, LB and M9.

526

527 ***In vitro* growth**

528 Overnight cultures of *Psa* NZ13^{kanR} and *Psa* NZ45 were used to determine
529 the *in vitro* growth of each strain in MGY alone or supplemented with 0.5 and
530 0.8mM CuSO₄. 10mL liquid MGY cultures were established with a starting
531 density of 10⁵ cfu mL⁻¹ and shaken for up to three days. Bacterial growth was
532 monitored by plating on KB kanamycin (*Psa* NZ13^{kanR}), MGY 0.8mM CuSO₄ (*Psa*
533 NZ45). Three replicates per strain and media combination was used, and the
534 experiment was repeated three times.

535

536 ***In planta* growth**

537 Clonally propagated *Actinidia chinensis* var. 'Hort16A' plantlets were
538 maintained at 20°C with a light/dark period of 14/10 hours, 70% constant
539 humidity. *Psa* NZ13^{kanR} and *Psa* NZ45 were grown on KB agar plates for 48h at
540 28°C. Inoculum with a final optical density (OD₆₀₀) of 0.2 of either strain was
541 prepared in 50 ml 10mM MgCl₂ with 0.002% of Silwet. Three to four week old
542 plantlets were inoculated by dipping the aerial parts in the inoculum solution for
543 5 seconds. Five separate plantlets were dip inoculated for each treatment. For
544 experiments assessing *in planta* growth in copper-sprayed plantlets, Nordox75
545 was used at the recommended dosage of 0.375g L⁻¹.

546 (www.kvh.org.nz/spray_products). Dip-inoculated plantlets were allowed to dry,

547 then sprayed adaxially and abaxially with Nordox75 until runoff to ensure
548 complete coverage. Bacterial growth was monitored 0, 3 and 7 days post
549 inoculation. 1 cm² disk leaves were cut using a sterile cork borer, surface
550 sterilized in 70% ethanol and ground in 200 µl 10mM MgCl₂. Serial dilutions of
551 the homogenate were plated on KB kanamycin to count *Psa* NZ13^{kanR} and MGY
552 0.8mM CuSO₄ to count *Psa* NZ45. Each experiment was repeated 3 times.

553

554 ***In vitro* and *in planta* competition assays**

555 *In vitro* and *in planta* competition assays were conducted as described
556 earlier for single strains, except that *Psa* NZ45 and *Psa* NZ13^{kanR} were
557 coinoculated in a 1:1 mix. Bacterial growth was monitored by plating serial
558 dilutions on KB kanamycin (*Psa* NZ13^{kanR}), MGY 0.8mM CuSO₄ (*Psa* NZ45) and on
559 MGY kanamycin 0.8mM CuSO₄ (*Psa* NZ13^{kanR} that acquired copper resistance). *In*
560 *vitro* assays had three replicates per strain, *in planta* assays were conducted
561 using five replicates, each experiment was repeated three times. Fitness was
562 calculated as ratio between their Malthusian Parameters (Lenski *et al.*, 1991).

563

564 **ICE integration screening**

565 Primers used in this study are listed in Supp Table 2. Four primers were
566 designed to detect the genomic location of ICE integration: two specific for the
567 integrases at the end of each ICEs (*IntPsaNZ45*, *IntPsaNZ13*) and two for the ICE
568 insertion site on the chromosome, annealing to the *clpB* (*att-1* site) and *queC*
569 (*att-2* site) genes. The primer combination (*IntPsaNZ45-att-2*, *IntPsaNZ45-att-1*,
570 *IntPsaNZ13-att-1*, and *IntPsaNZ13-att-2*) indicates the location of the ICEs.
571 Another two sets of primers were designed to amplify either CuR (*copA*) or

572 enolase genes present in the VR of *Psa*_{NZ45}ICE_Cu and *Psa*_{NZ13}ICE_eno,
573 respectively. PCRs were performed using Thermo Scientific *Taq DNA Polymerase*
574 following the manufacturer's instructions.

575

576 **ICE mobilization assay**

577 *Psa* NZ45 was used as the ICE donor. Strains tested in the mobilization
578 assays included are listed in order of divergence relative to the donor: *Psa* K28
579 (biovar 2) (McCann *et al.*, 2013), *Psa* J31 (biovar 1) (McCann *et al.*, 2013),
580 *Peusomonas syringae* pv. *actinidifoliorum* NZ9 (McCann *et al.*, 2013),
581 *Pseudomonas syringae* pv. *tomato* DC3000 (Buell *et al.*, 2003), *Pseudomonas*
582 *syringae* pv *phaseolicola* 1448a (Teverson, 1991), *Pseudomonas syringae* H24 and
583 H33 (isolated from kiwifruit; C. Straub, unpublished data), *Pseudomonas*
584 *fluorescens* SBW25 (Zhang *et al.*, 2006) and *Pseudomonas aeruginosa* PAO1
585 (Holloway, 1955). The copper sulphate MIC was determined for all tested
586 recipient strains, which were all tagged with kanamycin Tn5. A biparental
587 mating was performed using 2 mL and 200µl of washed recipient and *Psa* NZ45
588 cells, respectively. The cells were mixed, centrifuged briefly and resuspended in
589 30µl of 10 mM MgCl₂ alone, 10 mM MgCl₂ with 0.5mM CuSO₄ or 30 µl of 1 cm²
590 kiwifruit plantlet macerate in 200µl of 10 mM MgCl₂ if requested. The cell
591 mixture was plated onto solid media (M9 plates) and incubated at 28°C for 48
592 hours. Cells were then harvested and resuspended in 1ml of sterile 10 mM MgCl₂.
593 Serial dilutions were plated on KB kanamycin to count the total number of
594 recipients and on MGY amended with kanamycin and copper sulphate at
595 recipient MIC to count transconjugants.

596

597 **Biosecurity and approval**

598 All worked was performed in approved facilities and in accord with

599 APP201675, APP201730, APP202231.

600

601 **ACKNOWLEDGMENTS**

602 We gratefully acknowledge Zespri International Limited and Te Puke Fruit

603 Growers Association for financial support. The sponsors had no role in the

604 design, collation, or interpretation of data. We thank kiwifruit growers in Te

605 Puke for the access to orchards, Denis Robinson for providing Nordox75, and

606 Daniel Rexin for assistance with isolating *Psa* from kiwifruit leaves.

607

608 **REFERENCES**

609 Abelleira, A., López, M.M., Peñalver, J., Aguín, O., Mansilla, J.P., Picoaga, A. and

610 García, M.J. (2011) First report of bacterial canker of kiwifruit caused by

611 *Pseudomonas syringae* pv. *actinidiae* in Spain. Plant Dis 95: 1583.

612 Andersson, D.I. and Hughes, D. (2010) Antibiotic resistance and its cost: is it

613 possible to reverse resistance? Nature Reviews Microbiology 8: 260–271.

614 Aziz, R.K., Bartels, D., Best, A.A., DeJongh, M., Disz, T., Edwards, R.A. *et al.* (2008)

615 The RAST Server: rapid annotations using subsystems technology. BMC

616 Genomics 9: 75-10.1186/1471-2164-9-75.

617 Balestra, G.M., Renzi, M. and Mazzaglia, A. (2010) First report of bacterial canker

618 of *Actinidia deliciosa* caused by *Pseudomonas syringae* pv. *actinidiae* in

619 Portugal. New Dis Rep 22: 10.

620 Beaber, J.W., Hochhut, B. and Waldor, M.K. (2002) Genomic and functional

621 analyses of SXT, an integrating antibiotic resistance gene transfer element

- 622 derived from *Vibrio cholerae*. J Bacteriol 184: 4259–4269.
- 623 Bender, C.L. and Cooksey, D.A. (1986) Indigenous plasmids in *Pseudomonas*
624 *syringae* pv. *tomato*: conjugative transfer and role in copper resistance. J.
625 Bacteriol 165: 534-541.
- 626 Bondarczuk, K. and Piotrowska-Seget, Z. (2013) Molecular basis of active copper
627 resistance mechanisms in Gram-negative bacteria. Cell Biol Toxicol 29: 397–
628 405.
- 629 Buell, C.R., Joardar, V., Lindeberg, M., Selengut, J., Paulsen, I.T., Gwinn, M.L. *et al.*
630 (2003) The complete genome sequence of the Arabidopsis and tomato
631 pathogen *Pseudomonas syringae* pv. *tomato* DC3000. Proc Nat Acad Sci U S A
632 100: 10181–10186.
- 633 Burrus, V., Marrero, J. and Waldor, M.K. (2006) The current ICE age: biology and
634 evolution of SXT-related integrating conjugative elements. Plasmid 55: 173–
635 183.
- 636 Butler, M.I., Stockwell, P.A., Black, M.A., Day, R.C., Lamont, I.L. and Poulter, R.T.M.
637 (2013) *Pseudomonas syringae* pv. *actinidiae* from recent outbreaks of kiwifruit
638 bacterial canker belong to different clones that originated in China. PLoS ONE
639 8: e57464.
- 640 Cha, J.S. and Cooksey, D.A. (1993) Copper hypersensitivity and uptake in
641 *Pseudomonas syringae* containing cloned components of the copper resistance
642 operon. Appl Environ Microbiol 59: 1671–1674.
- 643 Dimopoulou, I.D., Kartali, S.I., Harding, R.M., Peto, T.E.A. and Crook, D.W. (2007)
644 Diversity of antibiotic resistance integrative and conjugative elements among
645 haemophili. J Med Microbiol 56: 838–846.
- 646 Ditta, G., Stanfield, S., Corbin, D., Helinski, D.R. (1980) Broad host range DNA

- 647 cloning system for gram-negative bacteria: construction of a gene bank of
648 *Rhizobium meliloti*. Proc Natl Acad Sci U S A 77: 7347–7351.
- 649 Drenkard, E. and Ausubel, F.M. (2002) *Pseudomonas* biofilm formation and
650 antibiotic resistance are linked to phenotypic variation. Nature 416: 740–743.
- 651 Everett, K.R., Taylor, R.K., Romberg, M.K., Rees-George, J., Fullerton, R.A.,
652 Vanneste, J.L. and Manning, M.A. (2011) First report of *Pseudomonas syringae*
653 pv. *actinidiae* causing kiwifruit bacterial canker in New Zealand. Australasian
654 Plant Dis Note 6: 67–71.
- 655 Fang, Y., Wu, L., Chen, G., Feng, G. (2016) Complete genome sequence of
656 *Pseudomonas azotoformans* S4, a potential biocontrol bacterium. J Biotechnol
657 227: 25-26.
- 658 Feil, H., Feil, W.S., Chain, P., Larimer, F., Di Bartolo, G., Copeland, A., *et al.* (2005)
659 Comparison of the complete genome sequences of *Pseudomonas syringae* pv.
660 *syringae* B728a and pv. *tomato* DC3000. Proc Natl Acad Sci U S A 102: 11064-
661 11069.
- 662 Fondi, M., Karkman, A., Tamminen, M.V., Bosi, E., Virta, M., Fani, R. *et al.* (2016)
663 “Every gene is everywhere but the environment selects”: global
664 geolocalization of gene sharing in environmental samples through network
665 analysis. Genome Biol Evol 8: 1388–1400.
- 666 Garriss, G., Waldor, M.K. and Burrus, V. (2009) Mobile antibiotic resistance
667 encoding elements promote their own diversity. PLoS Genetic 5: e1000775.
- 668 Guglielmini, J., Quintais, L., Garcillán-Barcia, M. P., de la Cruz, F., Rocha, E.P.
669 (2011) The repertoire of ICE in prokaryotes underscores the unity, diversity,
670 and ubiquity of conjugation. PLoS Genet 7: e1002222.
- 671 Gullberg, E., Albrecht, L.M., Karlsson, C., Sandegren, L. and Andersson, D.I. (2014)

672 Selection of a multidrug resistance plasmid by sublethal levels of antibiotics
673 and heavy metals. *mBio* 5: e01918–14.

674 Gutiérrez-Barranquero, J.A., de Vicente, A., Carrión, V.J., Sundin, G.W. and Cazorla,
675 F.M. (2013) Recruitment and rearrangement of three different genetic
676 determinants into a conjugative plasmid increase copper resistance in
677 *Pseudomonas syringae*. *Appl Environ Microbiol* 79: 1028–1033.

678 Holloway, B.W. (1955) Genetic recombination in *Pseudomonas aeruginosa*. *J Gen*
679 *Microbiol* 13: 572–581.

680 Johnson, C.M. and Grossman, A.D. (2015) Integrative and conjugative elements
681 (ICEs): what they do and how they work. *Annu Rev Genet* 49: 577–601.

682 Juhas, M., Power, P.M., Harding, R.M., Ferguson, D.J., Dimopoulou, I.D., Elamin,
683 A.R., *et al.* (2007) Sequence and functional analyses of *Haemophilus* spp.
684 genomic islands. *Genome Biol* 8: R237.

685 Kearse, M., Moir, R., Wilson, A., Stones-Havas, S., Cheung, M., Sturrock, S., *et al.*
686 (2012). Geneious Basic: an integrated and extendable desktop software
687 platform for the organization and analysis of sequence data. *Bioinformatics*
688 28: 1647-1649.

689 Kung, V.L., Ozer, E.A. and Hauser, A.R. (2010) The accessory genome of
690 *Pseudomonas aeruginosa*. *Microbiol Mol Biol Rev* 74: 621–641.

691 Lenski, R.E., Rose, M.R., Simpson, S.C. and Tadler, S.C. (1991) Long-term
692 experimental evolution in *Escherichia coli*. I. Adaptation and divergence
693 during 2,000 generations. *Am Nat* 138: 1315–1341.

694 Lilley, A.K., Bailey, M.J. (1997) Impact of plasmid pQBR103 acquisition and
695 carriage on the phytosphere fitness of *Pseudomonas fluorescens* SBW25:
696 burden and benefit. *Appl Environ Microbiol* 63: 1584–1587.

- 697 Lovell, H.C., Mansfield, J.W., Godfrey, S.A.C., Jackson, R.W., Hancock, J.T. and
698 Arnold, D.L. (2009). Bacterial evolution by genomic island transfer occurs via
699 DNA transformation *in planta*. *Curr Biol* 19: 1586–1590.
- 700 Mazzaglia, A., Studholme, D.J., Taratufolo, M.C., Cai, R., Almeida, N.F., Goodman, T.,
701 *et al.* (2012) *Pseudomonas syringae* pv. *actinidiae* (PSA) isolates from recent
702 bacterial canker of kiwifruit outbreaks belong to the same genetic lineage.
703 *PLoS One* 7: e36518.
- 704 Mergeay, M., Monchy, S., Vallaey, T., Auquier, V., Benotmane, A., Bertin, P., *et al.*
705 (2003) *Ralstonia metallidurans*, a bacterium specifically adapted to toxic
706 metals: towards a catalogue of metal-responsive genes. *FEMS Microbiol Rev*
707 27: 385–410.
- 708 McCann, H.C., Rikkerink, E.H.A., Bertels, F., Fiers, M., Lu, A., Rees-George, J., *et al.*
709 (2013) Genomic analysis of the kiwifruit pathogen *Pseudomonas syringae* pv.
710 *actinidiae* provides insight into the origins of an emergent plant disease. *PLoS*
711 *Pathogens* 9: e1003503.
- 712 McCann, H.C., Li, L., Liu, Y., Templeton, M.D., Colombi, E., Straub, C., *et al.* (2016)
713 The origin and evolution of a pandemic lineage of the kiwifruit pathogen
714 *Pseudomonas syringae* pv. *actinidiae*. In review.
- 715 Mohd-Zain, Z., Turner, S.L., Cerdano-Tarraga, A.M., Lilley, A.K., Inzana, T.J.,
716 Duncan, A.J., *et al.* (2004) Transferable antibiotic resistance elements in
717 *Haemophilus influenzae* share a common evolutionary origin with a diverse
718 family of syntenic genomic islands. *J Bacteriol*, 186: 8114–8122.
- 719 Morgan, R.K. and Taylor, E. (2004) Copper accumulation in vineyard soils in New
720 Zealand. *Environ Sci* 1:2, 139-167.
- 721 Nakajima, M., Goto, M. and Hibi, T. (2002) Similarity between copper resistance

- 722 genes from *Pseudomonas syringae* pv. *actinidiae* and *P. syringae* pv. *tomato*, J
723 Gen Plant Pathol 68: 68–74.
- 724 Neale, H. C., Laister, R., Payne, J., Preston, G., Jackson, R. W. and Arnold, D. L.
725 (2016) A low frequency persistent reservoir of a genomic island in a pathogen
726 population ensures island survival and improves pathogen fitness in a
727 susceptible host. Environ Microbiol *Accepted Author Manuscript*.
728 doi:10.1111/1462-2920.13482
- 729 Ochman, H., Lerat, E., Daubin, V. (2005) Examining bacterial species under the
730 specter of gene transfer and exchange. Proc Natl Acad Sci U S A 102 Suppl 1:
731 6595-6599.
- 732 Ochman, H., Lawrence, J.G. and Groisman, E.A. (2010) Lateral gene transfer and
733 the nature of bacterial innovation. Nature 405: 299–304.
- 734 Peters, S.E., Hobman, J.L., Strike, P. and Ritchie, D.A. (1991) Novel mercury
735 resistance determinants carried by IncJ plasmids pMERPH and R391. Mol Gen
736 Genet 228: 294–299.
- 737 Pitman, A.R., Jackson, R.W., Mansfield, J.W., Kaitell, V., Thwaites, R., *et al.* (2005)
738 Exposure to host resistance mechanisms drives evolution of bacterial
739 virulence in plants. Curr Biol 15: 2230–2235.
- 740 Polz, M.F., Alm, E.J., and Hanage, W.P. (2013) Horizontal gene transfer and the
741 evolution of bacterial and archaeal population structure. Trends Genet 29:
742 170–175.
- 743 Quiroz, T.S., Nieto, P.A., Tobar, H.E., Salazar-Echegarai, F.J., Lizana, R.J., Quezada
744 C.P., *et al.* (2011) Excision of an unstable pathogenicity island in *Salmonella*
745 *enterica* serovar *enteritidis* is induced during infection of phagocytic cells.
746 PLoS ONE 6: e26031.

- 747 Ramsay, J.P., Sullivan, J.T., Stuart, G.S., Lamont, I.L. and Ronson, C.W. (2006)
748 Excision and transfer of the *Mesorhizobium loti* R7A symbiosis island requires
749 an integrase IntS, a novel recombination directionality factor RdfS, and a
750 putative relaxase RlxS. *Mol Microbiol* 62: 723–734.
- 751 Rauch, P.J.G. and De Vos, W.M. (1992) Characterization of the novel nisin-sucrose
752 conjugative transposon Tn5276 and its insertion in *Lactococcus lactis*. *J*
753 *Bacteriol* 174: 1280-1287.
- 754 Ravatn, R., Studer, S., Springael, D., Zehnder, A.J.B. and Van Der Meer, J.R. (1998)
755 Chromosomal integration, tandem amplification, and deamplification in
756 *Pseudomonas putida* F1 of a 105-kilobase genetic element containing the
757 chlorocatechol degradative genes from *Pseudomonas* sp. strain B13. *J Bacteriol*
758 180: 4360–4369.
- 759 Rees-George, J., Vanneste, J.L., Cornish, D.A., Pushparajah, I.P.S., Yu, J., Templeton,
760 M.D. and Everett, K.R. (2010) Detection of *Pseudomonas syringae* pv. *actinidiae*
761 using polymerase chain reaction (PCR) primers based on the 16S-23S rDNA
762 intertranscribed spacer region and comparison with PCR primers based on
763 other gene regions. *Plant Pathol* 59: 453–464.
- 764 Rensing, C. and Grass, G. (2003) *Escherichia coli* mechanisms of copper
765 homeostasis in a changing environment. *FEMS Microbiol Rev* 27: 197–213.
- 766 Roberts, A.P. and Mullany, P. (2009) A modular master on the move: the Tn916
767 family of mobile genetic elements. *Trends Microbiol* 17: 251–258.
- 768 Ruinelli, M., Schneeberger, P.H.H., Ferrante, P., Bühlmann, A., Scortichini, M.,
769 Vanneste, J.L., *et al.* (2016) Comparative genomics-informed design of two
770 LAMP assays for detection of the kiwifruit pathogen *Pseudomonas syringae* pv.
771 *actinidiae* and discrimination of isolates belonging to the pandemic biovar 3.

- 772 Plant Pathol doi:10.1111/ppa.12551.
- 773 Staehlin, B.M., Gibbons, J.G., Rokas, A., O'Halloran, T.V. and Slot, J.C. (2016)
- 774 Evolution of a heavy metal homeostasis/resistance island reflects increasing
- 775 copper stress in *Enterobacteria*. *Genome Biol Evol* 8: 811-826.
- 776 Stoesser, N., Giess, A., Batty, E.M., Sheppard, A.E., Walker, A.S., Wilson, D.J., *et al.*
- 777 (2014) Genome sequencing of an extended series of NDM-producing *Klebsiella*
- 778 *pneumoniae* isolates from neonatal infections in a Nepali hospital
- 779 characterizes the extent of community- versus hospital-associated
- 780 transmission in an endemic setting. *Antimicrob Agents Chemother* 58: 7347–
- 781 7357.
- 782 Sullivan, J.T., Patrick, H.N., Lowther, W.L., Scott, D.B. and Ronson, C.W. (1995)
- 783 Nodulating strains of *Rhizobium loti* arise through chromosomal symbiotic
- 784 gene transfer in the environment. *Proc Natl Acad Sci USA* 92: 8985–8989.
- 785 Sullivan, J.T. and Ronson, C.W. (1998) Evolution of rhizobia by acquisition of a
- 786 500-kb symbiosis island that integrates into a phe-tRNA gene. *Proc Natl Acad*
- 787 *Sci USA* 95: 5145–514.
- 788 Templeton, M.D., Warren, B.A., Andersen, M.T., Rikkerink, E.H.A., Fineran, P.C.
- 789 (2015) Complete DNA sequence of *Pseudomonas syringae* pv. *actinidiae*, the
- 790 causal agent of kiwifruit canker disease. *Genome Announc* 3: e01054-15.
- 791 Teverson, D.M. (1991) Genetics of pathogenicity and resistance in the halo-blight
- 792 disease of beans in Africa. Ph.D. thesis. University of Birmingham,
- 793 Birmingham, United Kingdom.
- 794 Vanga, B.R., Ramakrishnan, P., Butler, R.C., Toth, I.K., Ronson, C.W., Jacobs, J.M.E.
- 795 and Pitman, A.R. (2015) Mobilization of horizontally acquired island 2 is
- 796 induced in plantain the phytopathogen *Pectobacterium atrosepticum*

797 SCRI1043 and involves the putative relaxase ECA0613 and quorum sensing.
798 Environ Microbiol 17: 4730–4744.

799 Vanneste, J.L., Giovanardi, D., Yu, J., Cornish, D.A., Kay, C., Spinelli, F. and Stefani,
800 E. (2011) Detection of *Pseudomonas syringae* pv. *actinidiae* in kiwifruit pollen
801 samples. N Z Plant Protect 64: 246-251.

802 Visnovsky, S.B., Fiers, M., Lu, A., Panda, P., Taylor, R. and Pitman, A.R. (2016)
803 Draft genome sequences of 18 strains of *Pseudomonas* isolated from kiwifruit
804 plants in New Zealand and overseas. Genome Announc 4: e00061–16.

805 Wozniak, R.A.F. and Waldor, M.K. (2010) Integrative and conjugative elements:
806 mosaic mobile genetic elements enabling dynamic lateral gene flow. Nat Rev
807 Microbiol 8: 552–563.

808 Zhang, X.X., Gauntlett, J.C., Oldenburg, D.G., Cook, G.M. and Rainey, P.B. (2015)
809 role of the transporter-like sensor kinase CbrA in histidine uptake and signal
810 transduction. J Bacteriol 197: 2867–2878.

811 Zhang, X.X., George, A., Bailey, M.J. and Rainey, P.B. (2006) The histidine
812 utilization (*hut*) genes of *Pseudomonas fluorescens* SBW25 are active on plant
813 surfaces, but are not required for competitive colonization of sugar beet
814 seedlings. Microbiol 152: 1867–1875.

815

816 **TABLE AND FIGURE**

817

818

819

820

821

822

823

824

825

826

827

828

829

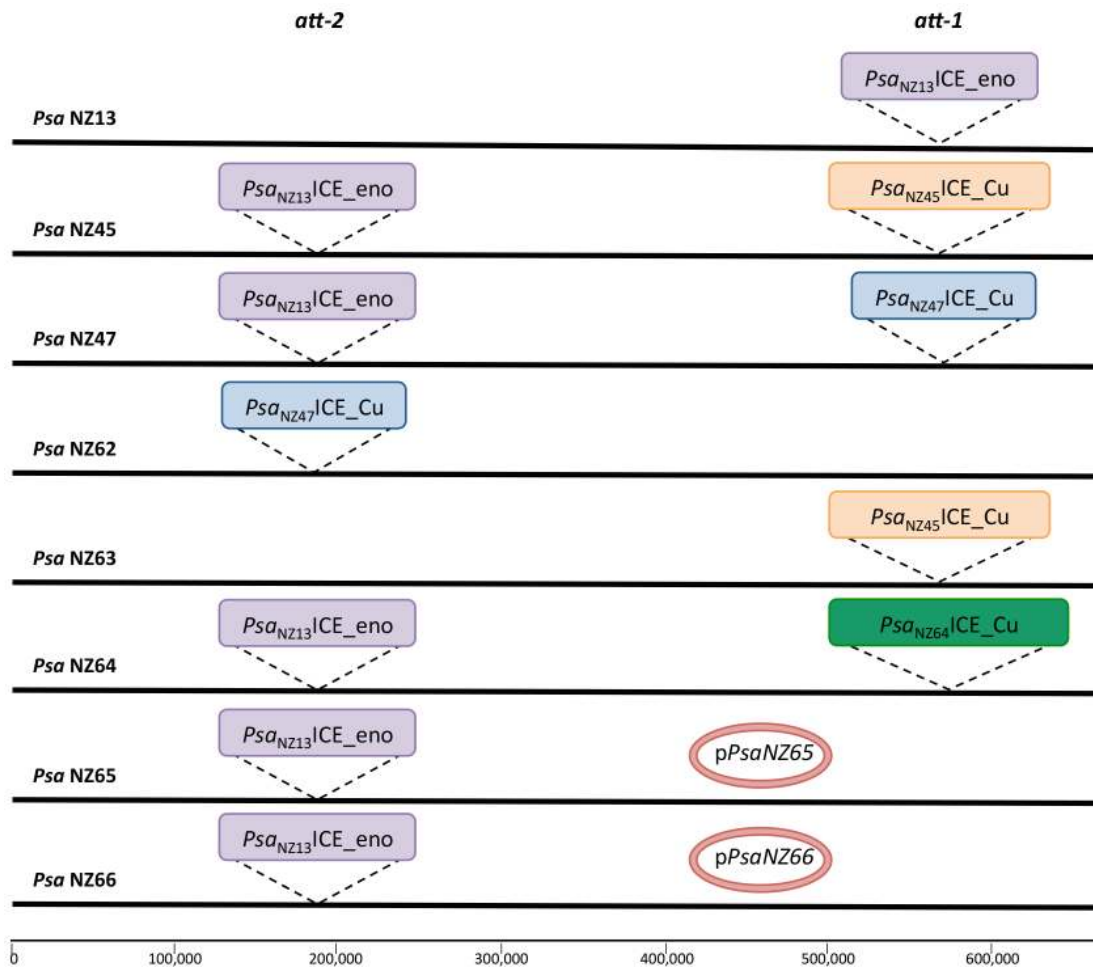
830

831

Isolate ID	Place of Isolation	Year of Isolation	Host of Isolation	Orchard's copper Programme	MIC to CuSO ₄	GenBank Accession	ICMP number
<i>Fsa</i> NZ13	Te Puke, NZ	2010	Kiwifruit	NA	0.8 mM	CP011972.1	18884
<i>Fsa</i> NZ45	Te Puke, NZ	2014	Kiwifruit	Full spray	1.2 mM	XXXX1	20586
<i>Fsa</i> NZ47	Te Puke, NZ	2014	Kiwifruit	Spray free	1.2 mM	XXXX2	22180
<i>Fsa</i> NZ62	Te Puke, NZ	2015	Kiwifruit	Organic	1.2 mM	XXXX3	22181
<i>Fsa</i> NZ63	Te Puke, NZ	2015	Kiwifruit	To minimum	1.2 mM	XXXX4	22182
<i>Fsa</i> NZ64	Te Puke, NZ	2016	Kiwifruit	Spray free	1.2 mM	XXXX5	22183
<i>Fsa</i> NZ65	Te Puke, NZ	2016	Kiwifruit	Full spray	1.5 mM	XXXX6	22184
<i>Fsa</i> NZ66	Coromandel, NZ	2016	Kiwifruit	Full spray	1.5 mM	XXXX7	22185
<i>Fpa</i> LGM2367	Madison, USA	1921-1922	Proso millet	NA	NA	ALACO1000019.1 ALACO1000062.1	
<i>Fpf</i> ICMP4394	Auckland, NZ	1968	Wheat	NA	NA	LJP001000111.1 LJP001000188.1	4394
<i>P. manginialis</i> ICMP4394	Katikati, NZ	1991	Kiwifruit	NA	NA	LKGR010000860.1	4394
<i>Fsa</i> 12	Japan	1988	Kiwifruit	NA	NA	AGNQ01000195	
<i>Ffm</i> ICMP19497	Te Puke, NZ	2010	Kiwifruit	NA	NA	LKEQ01000112.1	19497

832 **Table 1. List of genomes used in this study.**

833



834

835 **Figure 1. Genomic location of *Psa*ICEs in *Psa* NZ13.** In purple the

836 *Psa*_{NZ13}|ICE_eno (100 kb), in orange *Psa*_{NZ45}|ICE_Cu (107 kb), in blue the

837 *Psa*_{NZ47}|ICE_Cu (90 kb), in green the *Psa*_{NZ64}|ICE_Cu (130 kb), p*Psa*NZ65 and

838 p*Psa*NZ66 plasmids are 111 kb. Each island is bounded by 52 bp *att* sequences

839 overlapping tRNA^{Lys}. In *Psa* NZ13 the *att-1* site is located at 5,534,632 bp, *att-2*

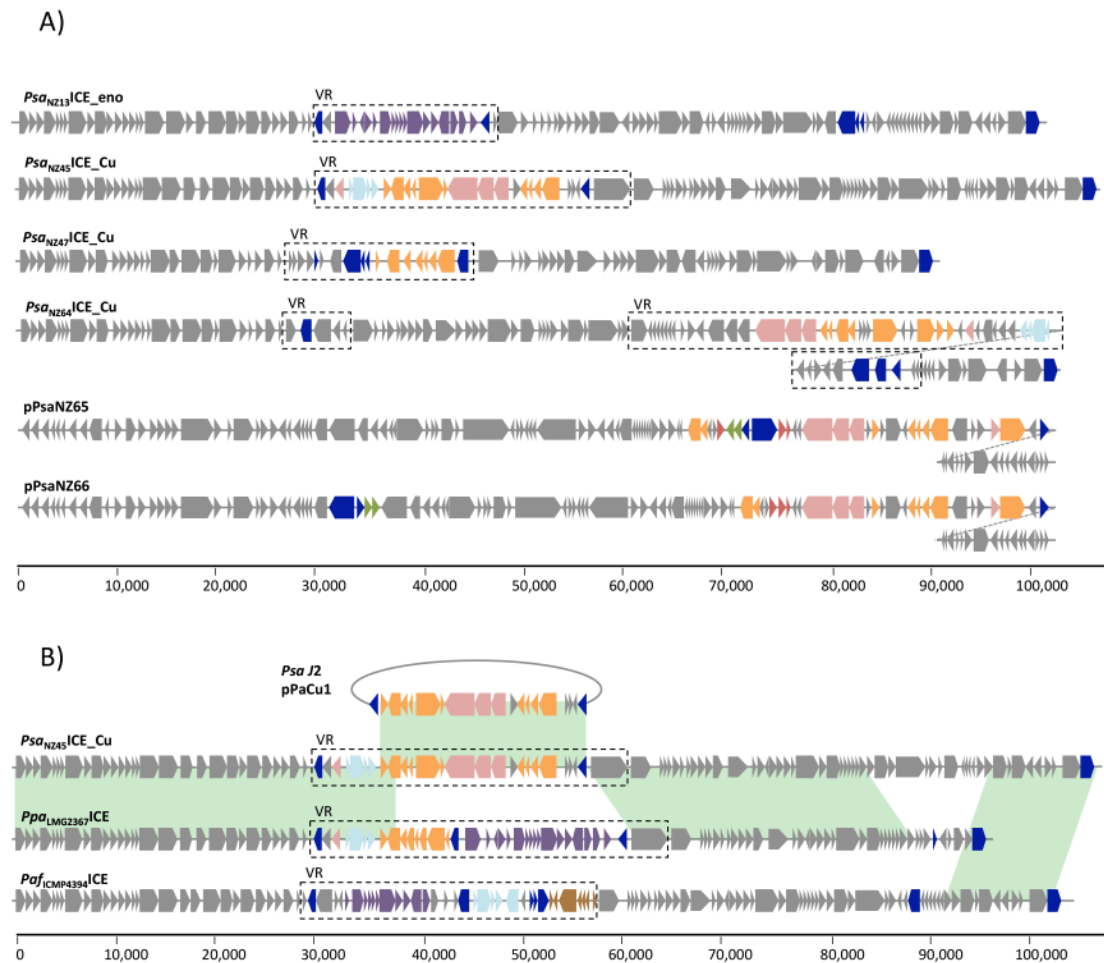
840 at 1,733,972 bp. The figure is not to scale (the entire genome of 6.7 Mbp is

841 indicated a single black line). Both *Psa*_{NZ13}|ICE_Eno and *Psa*_{NZ47}|ICE_Cu ICEs were

842 detected in *Psa* NZ47 by sequencing, but analysis of independent colonies from

843 the freezer stock show that *Psa*_{NZ13}|ICE_Eno is prone to loss.

844



845

846 **Figure 2. Genetic organization of ICEs and plasmids acquired by *Psa* and**

847 **mosaicism of *Psa*_{NZ45}ICE_Cu.**

848 **A)** Blue boxes are mobile genes (transposases or recombinases), purple boxes
849 define the 'enolase region', orange boxes depict copper resistance genes, azure
850 boxes are arsenic resistance genes, pink boxes are genes belonging to the *czc/cus*
851 system, green boxes are streptomycin resistance genes, red boxes are cation
852 transporter ATPases, brown boxes denote genes encoding mercury resistance.

853 Core "backbone" and other cargo genes are depicted as grey boxes. Dotted

854 diagonal lines indicate continuation of the element.

855 **B)** Areas in green show more than 99% pairwise nucleotide identity.

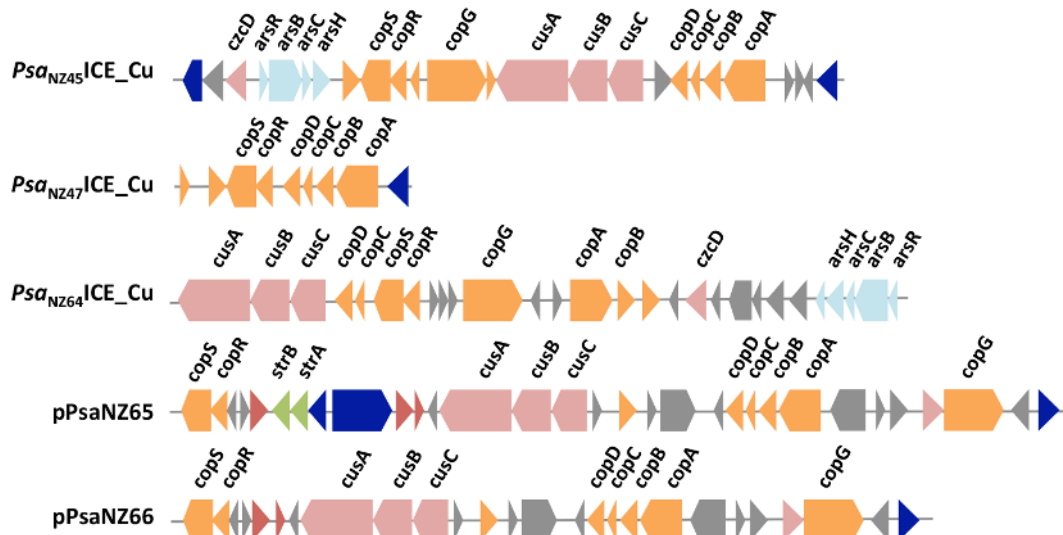
856 *Psa*_{NZ45}ICE_Cu and *Ppa*_{LGM2367}ICE share identity both in the first 38 kb and 20 kb

857 downstream of VR. The remaining 20 kb of the *Psa*_{NZ45}ICE_Cu VR is almost

858 identical to pPaCu1 (it differs by just 2 SNPs). The last 12.5 kb of *Psa*_{NZ45}ICE_Cu is

859 identical to *Paf*_{ICMP4394}ICE.

860



861

862

863 **Figure 3. Genetic organization of metal resistance loci.** Blue boxes are mobile

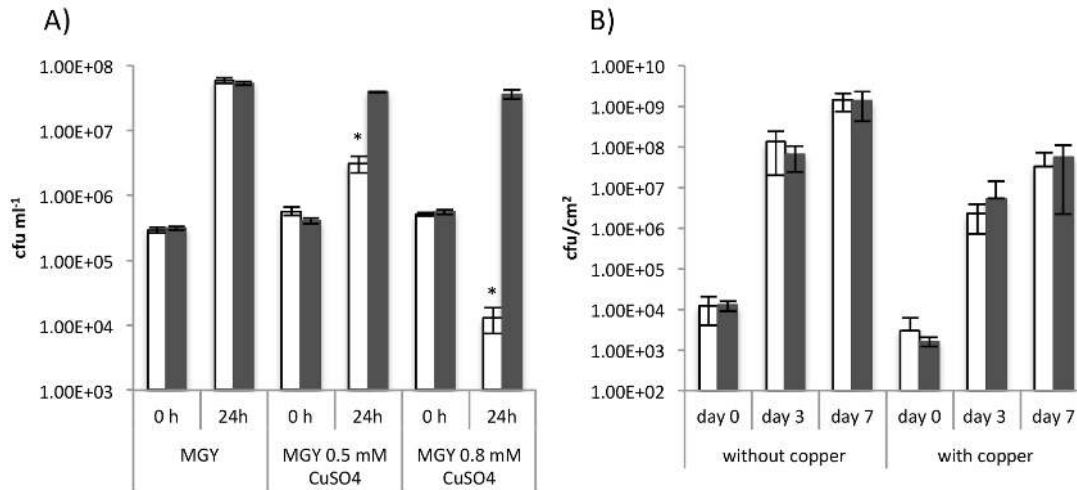
864 genes (transposases or recombinases), orange boxes depict copper resistance

865 genes, azure boxes are arsenic resistance genes, pink boxes are genes belonging

866 to the *czc/cus* system, green boxes are streptomycin resistance genes and other

867 genes are depicted as grey boxes.

868



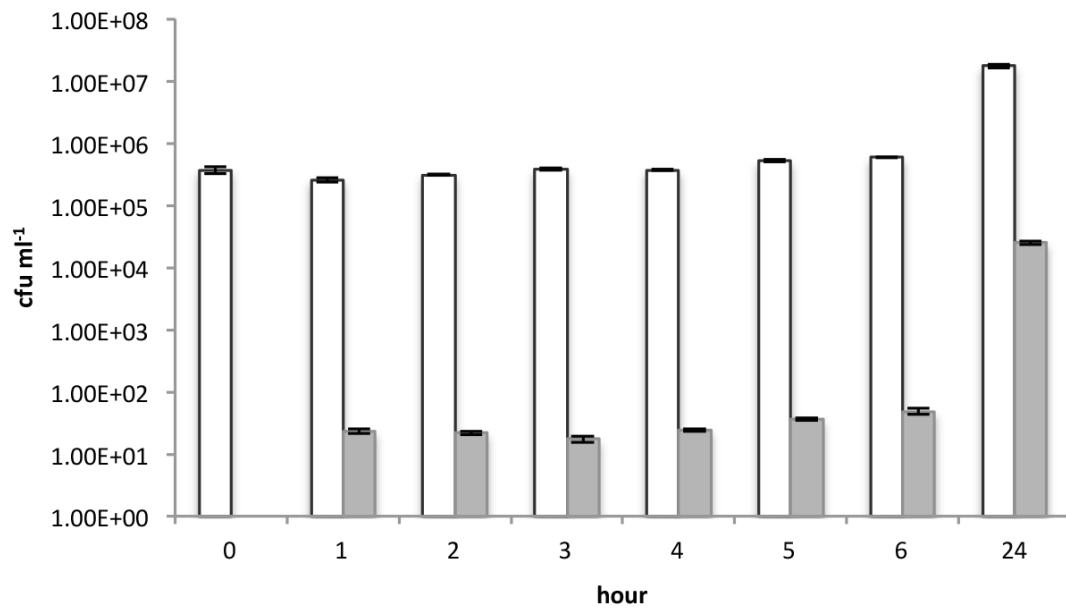
869

870 **Figure 4. Effect of copper ions on growth of *Psa* NZ13 and *Psa* NZ45.**

871 **A)** *Psa* NZ13 (white bars) and *Psa* NZ45 (grey bars) were grown for 24 h in
872 shaken MGY culture and MGY supplemented with 0.5mM and 0.8 mM CuSO₄.
873 Data are means and standard deviation of three independent cultures. *indicates
874 significant difference $P < 0.05$ (one tailed t -test)).

875 **B)** The single growth of *Psa* NZ13 (white bars) and *Psa* NZ45 (grey bars) was
876 assessed endophytically on leaves of the kiwifruit cultivar Hort16A. Data are
877 means and standard deviation of five replicates. The copper product Nordox75
878 (0.375g L⁻¹) was sprayed adaxially and abaxially until run off. Data are means
879 and standard deviation of 5 replicates. One tailed t -test showed no statistical
880 difference in growth between of *Psa* NZ13 and NZ45 in absence or presence of
881 copper.

882



883

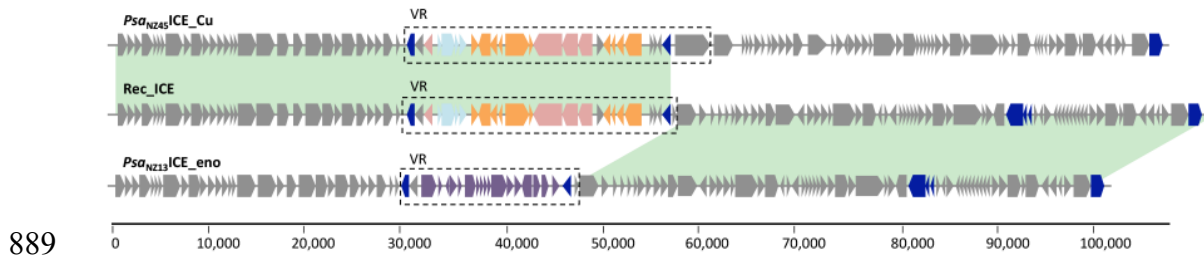
884 **Figure 5. *In vitro* transfer of *Psa*_{NZ45}ICE_Cu from *Psa* NZ45 to *Psa* NZ13.**

885 Colony forming units of the recipient *Psa* NZ13 (white bars) and *Psa* NZ13

886 carrying *Psa*_{NZ45}ICE_Cu (transconjugants, grey bars) was monitored during co-

887 cultivation. Data are means and standard deviation of 3 independent cultures

888



889

890 **Figure 6. Structure and mosaicism of the recombinant ICE (Rec_ICE) in**

891 **transconjugant *Psa* NZ13.** Areas highlighted in green show 100% pairwise

892 identity. The recombination break point is inside the variable region (VR). Blue

893 boxes are mobile genes (transposases or recombinases), purple boxes define the

894 'enolase region' (McCann *et al.* 2013), orange boxes depict copper resistance

895 genes, azure boxes are arsenic resistance genes and pink boxes are genes

896 belonging to the *czc/cus* system. Core "backbone" and other cargo genes are

897 depicted as grey boxes.

898

899

900

901

902

903

904

905

906

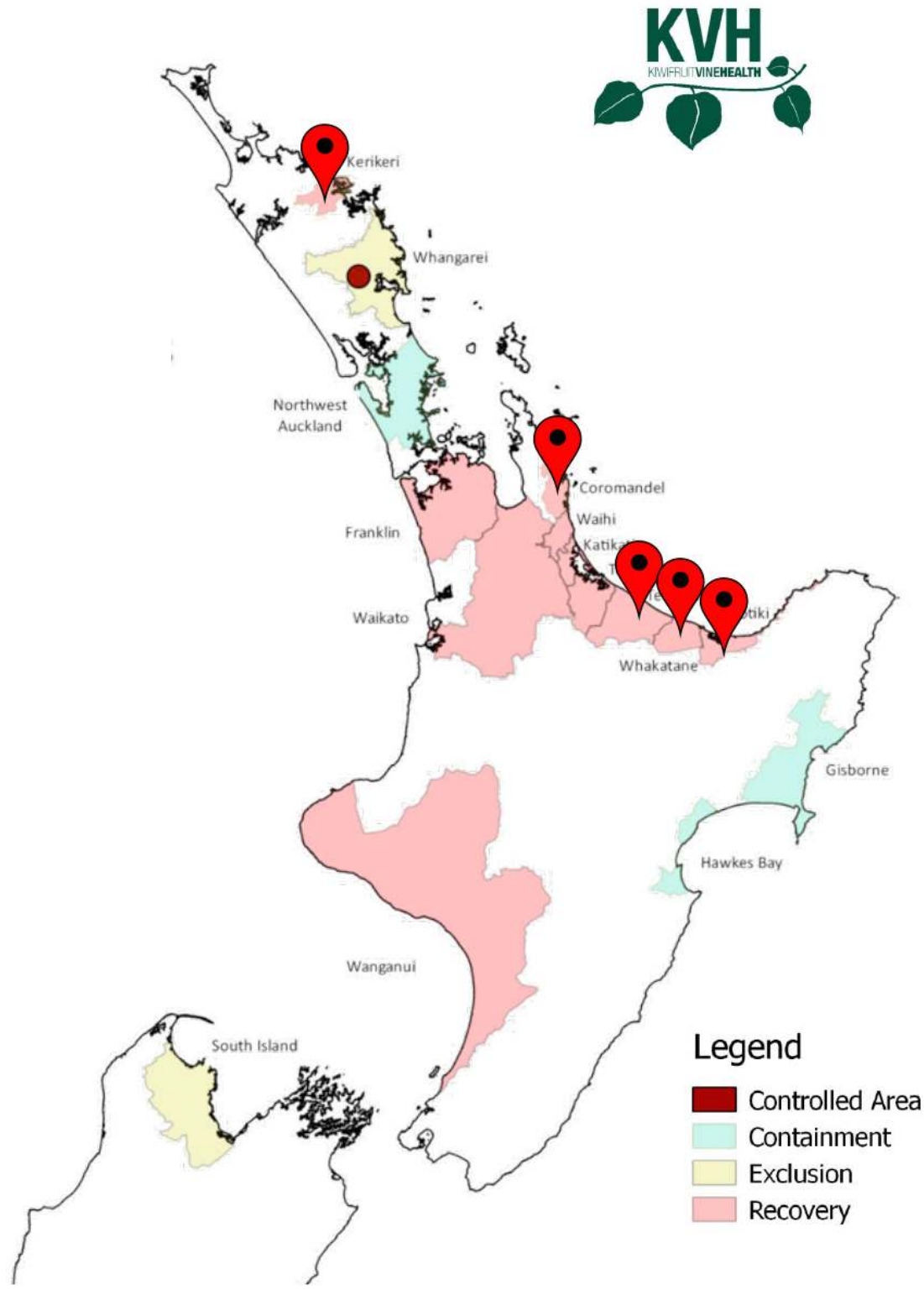
907

908

909

910

911 SUPPORTING INFORMATION

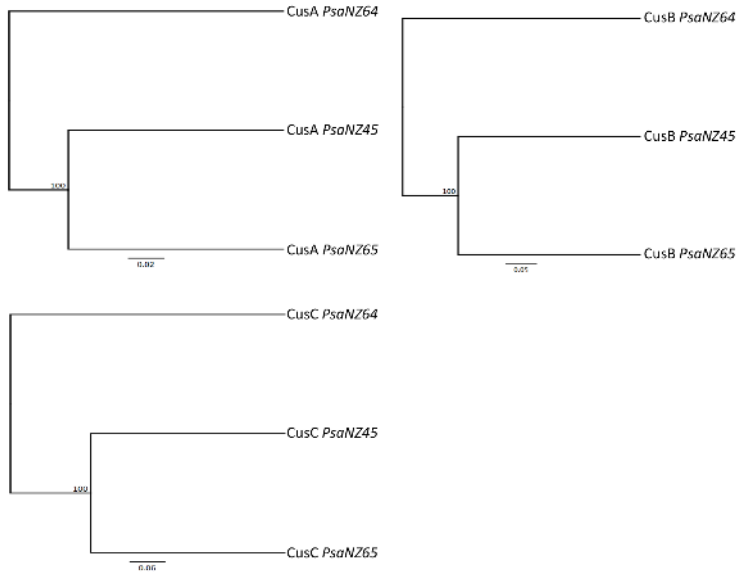


912

913 **Figure S1** – New Zealand kiwifruit growing regions with isolation sites of copper

914 resistant *Psa*. Map was modified from regional classification map of June 2016

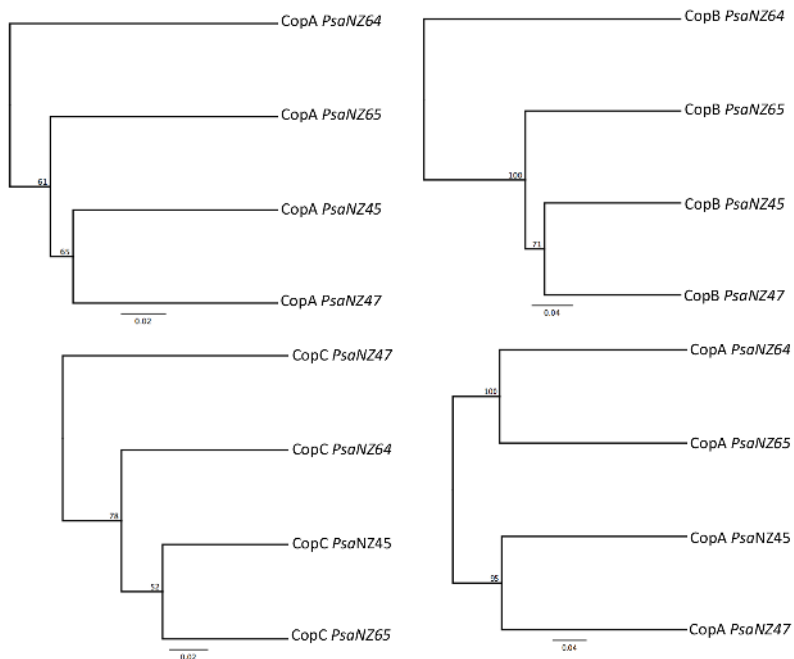
915 (Kiwi Vine Health (KVVH)).



916

917 **Figure S2 - UPMGA tree of the Cus system proteins in *Psa* NZ.** Bootstrap

918 values are shown at each node.



919

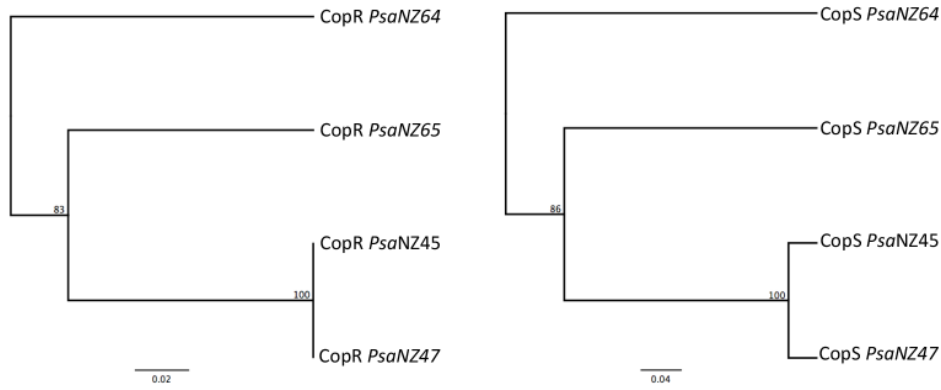
920 **Figure S3 - UPMGA trees of the Cop proteins genes in *Psa* NZ.** Bootstrap

921 values are shown at each node.

922

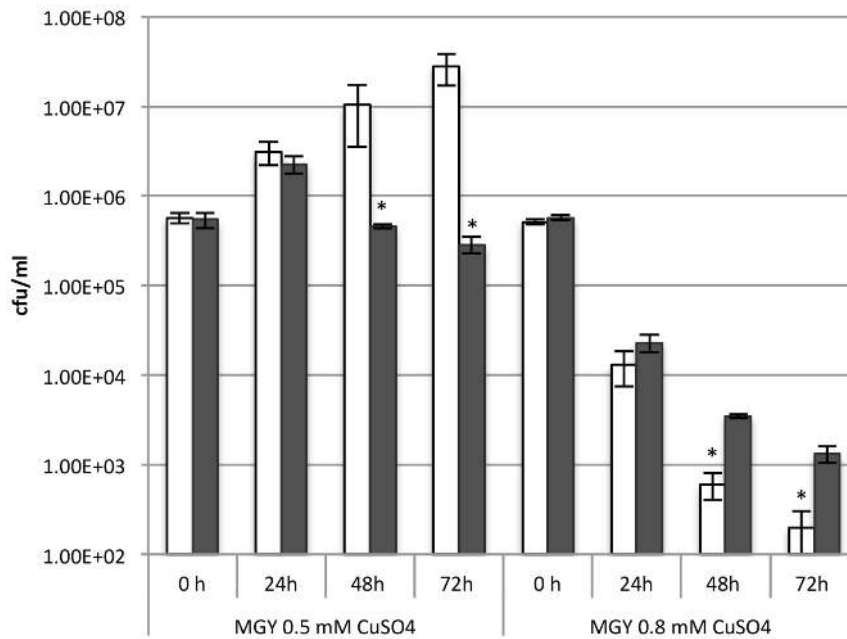
923

924



926 **Figure S4 - UPMGA trees of CopR and CopS proteins in *Psa NZ*.** Bootstrap
927 values are shown at each node.

928



930 **Figure S5. Density of single and co-cultured *Psa* in liquid MGY**

931 **supplemented with 0.5 mM and 0.8 mM CuSO₄.** *Psa NZ13* was cultured alone
932 (white bars) or co-cultured with *Psa NZ45* (grey bars). Data are means and
933 standard deviation of three independent cultures. *indicates significance at 5%
934 level by one-tailed *t*-test.

935

936

	Frequency of <i>Psa</i> _{NZ45} ICE_Cu transconjugants	
<i>Psa</i> NZ13 : <i>Psa</i> NZ45	day 3	day 7
1 : 1	$(2.05 \pm 0.63)^{-2}$	$(2.28 \pm 0.7)^{-2}$
1 : 0.1	$(1.34 \pm 0.52)^{-2}$	$(3.14 \pm 2.3)^{-2}$
0.1 : 1	$(1.68 \pm 0.68)^{-2}$	$(1.88 \pm 0.81)^{-2}$

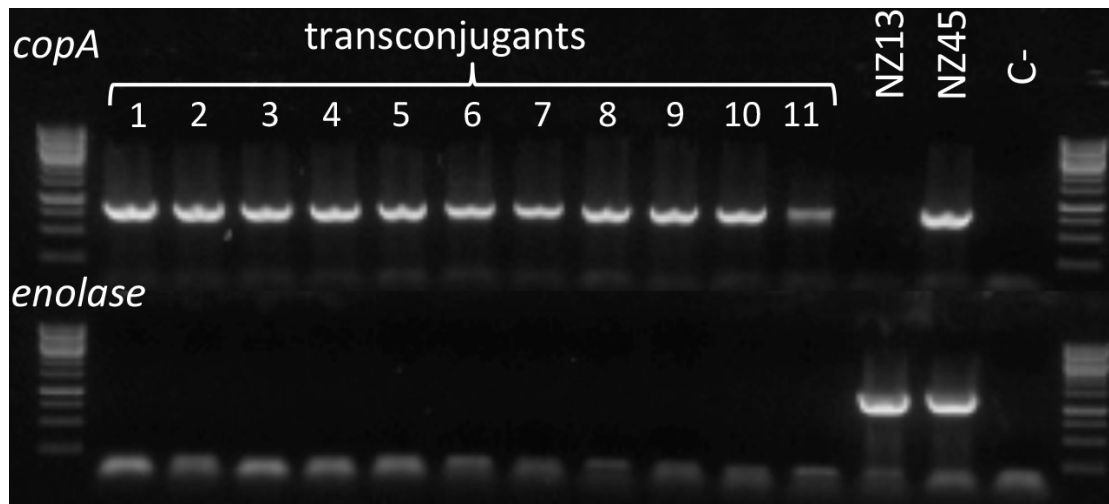
937

938 **Table S1. *In planta* transfer of *Psa*_{NZ45}ICE_cu from *Psa* NZ45 to *Psa* NZ13 at**
 939 **different founding ratios of donor and recipient.** Donor and recipient strains
 940 were dip-inoculated onto Hort16A leaves at different founding ratios and
 941 frequency of recipients determined at days 3 and 7

Primer name	Sequence
<i>copA for</i>	ATCCGCGGTGACTCGATAAC
<i>copA rev</i>	CAGTCGATGGACCGTACTGG
<i>enolase for</i>	GAGCTGACGTCCGACATAGAG
<i>enolase rev</i>	CCAGTCCAACAGGTTTACCG
<i>IntPsaNZ13</i>	GTCAGGCTGATCACTTACGTTG
<i>IntPsaNZ45</i>	GTCAGGCTGATCACTAGCGTTA
<i>att-1</i>	TGTAGAATAGCGCGCCTCAG
<i>att-2</i>	AGCCGTAATCCTGCTGTCC

942

943 **Table S2. Primers used for *Psa*_{NZ13}ICE_eno and *Psa*_{NZ45}ICE_Cu detection and**
 944 **integration loci.**



945

946

947 **Figure S6. Analysis of the presence of the variable region (VR) of**

948 ***Psa*_{NZ45}ICE_Cu and *Psa*_{NZ13}ICE_eno in 11 *Psa* NZ13 transconjugants.** PCRs

949 were carried out to detect *copA* (VR of *Psa*_{NZ45}ICE_Cu) or *enolase* genes (VR of

950 *Psa*_{NZ13}ICE_eno). Controls of *Psa* NZ13 and *Psa* NZ45 show one and two bands,

951 indicative of *Psa*_{NZ13}ICE_eno in *Psa* NZ13 and both *Psa*_{NZ13}ICE_eno *Psa*_{NZ45}ICE_Cu

952 and in *Psa* NZ45, respectively. All transconjugants, lanes 1-11 have acquired

953 *Psa*_{NZ45}ICE_Cu.

954

955

956

957

958

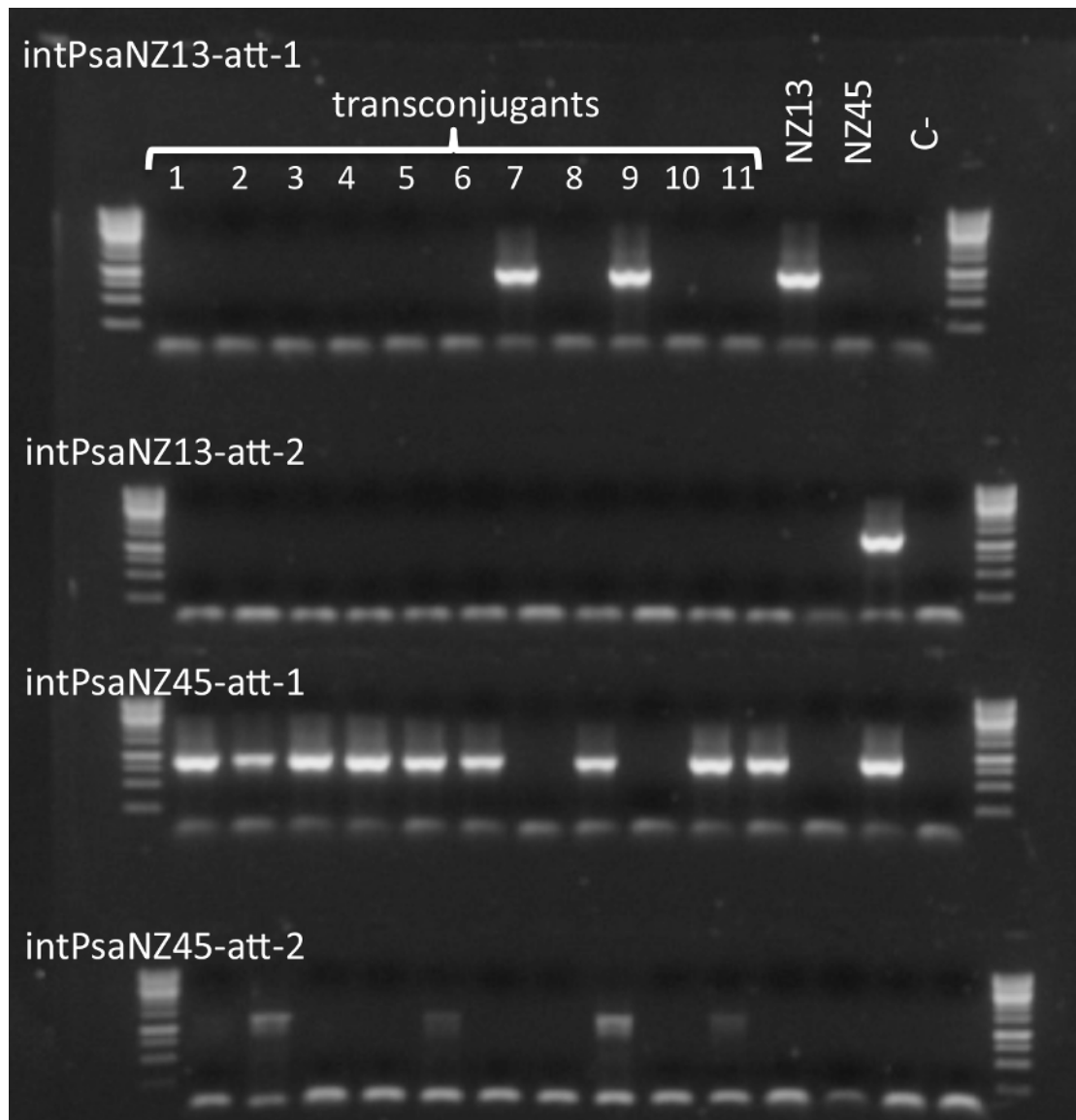
959

960

961

962

963



964

965 **Figure S7. Analysis of the insertion site of the *Psa*_{NZ13}ICE_eno and**
966 ***Psa*_{NZ45}ICE_Cu in 11 *Psa* NZ13 transconjugants.** PCRs were to detect the
967 integration of *Psa*_{NZ13}ICE_eno in the *att-1* or *att-2* sites (*intPsa*_{NZ13}-*att-1* and
968 *intPsa*_{NZ13}-*att-2*) and the integration of *Psa*_{NZ45}ICE_Cu in the *att-1* or *att-2* sites
969 (*intPsa*_{NZ45}-*att-1* and *intPsa*_{NZ45}-*att-2*). Controls of *Psa* NZ13 and *Psa* NZ45
970 show that in *Psa* NZ13 the *Psa*_{NZ13}ICE_eno is integrated in the *att-1* site and in
971 *Psa* NZ45 the *Psa*_{NZ13}ICE_eno is integrated in the *att-1* and the *Psa*_{NZ45}ICE_Cu in
972 the *att-2* site.